

# Preheating with non-minimally coupled scalar fields in higher-curvature inflation models

Shinji Tsujikawa<sup>1\*</sup>, and Kei-ichi Maeda<sup>1,2†</sup>

<sup>1</sup> *Department of Physics, Waseda University, Shinjuku, Tokyo 169-8555, Japan*

<sup>2</sup> *Advanced Research Institute for Science and Engineering,  
Waseda University, Shinjuku, Tokyo 169-8555, Japan*

Takashi Torii<sup>‡</sup>

*Department of Physics, Tokyo Institute of Technology, Meguro, Tokyo 152, Japan*

(October 26, 2019)

In higher-curvature inflation models ( $R + \alpha_n R^n$ ), we study a parametric preheating of a scalar field  $\chi$  coupled non-minimally to a spacetime curvature  $R$  ( $\xi R\chi^2$ ). In the case of  $R^2$ -inflation model, efficient preheating becomes possible for rather small values of  $\xi$ , i.e.  $|\xi| \lesssim$  several. Although the maximal fluctuation  $\sqrt{\langle \chi^2 \rangle_{max}} \approx 2 \times 10^{17}$  GeV for  $\xi \approx -4$  is almost the same as the chaotic inflation model with a non-minimally coupled  $\chi$  field, the growth rate of the fluctuation becomes much larger and efficient preheating is realized. We also investigate preheating for  $R^4$  model and find that the maximal fluctuation is  $\sqrt{\langle \chi^2 \rangle_{max}} \approx 8 \times 10^{16}$  GeV for  $\xi \approx -35$ .

98.80.Cq, 05.70.Fh, 11.15.Kc

## I. INTRODUCTION

The inflation is one of the most promising models for the early stage of the Universe in modern cosmology [1]. It not only gives a natural explanation for the horizon, flatness, and monopole problem but also provides us density perturbations as seeds for a large scale structure in the Universe [2]. So far, there are several models for inflation, i.e. a new inflation proposed by Albrecht and Steinhardt [3], and Linde [4], a chaotic inflation by Linde [5], and a higher-curvature inflation by Starobinsky [6]. The first two models require a scalar field which is called *inflaton* to drive inflation. The chaotic inflation scenario would be natural in the sense that initial conditions for inflation are not restricted so much as compared with a new inflation. On the other hand, the third model is based on adding the higher-curvature terms to the Einstein-Hilbert action. This model is remarkable in the sense that we have an inflationary solution without an inflaton scalar field. That is, inflation can be realized by purely gravitational coupling. Several authors [7] studied some constraints of coupling with higher-curvature and investigated its various aspects such as the cosmic no-hair theorem.

---

\*electronic address: shinji@gravity.phys.waseda.ac.jp

†electronic address: maeda@gravity.phys.waseda.ac.jp

‡electronic address: torii@th.phys.titech.ac.jp

An inflationary period will end when kinetic energy of an inflaton dominates over its potential energy. At this stage, the inflaton field begins to oscillate coherently around the minimum of its potential. The energy of the inflaton field will eventually be transferred to radiation, and this process is called reheating. The original version of the reheating scenario was considered in Ref. [8] just after the new inflation model is proposed. This old scenario is based on perturbation theory, adding a phenomenological decay term to the inflaton equation. Since the reheating temperature is constrained to be relatively small such as  $T_r \lesssim 10^9$  GeV and a production of GUT scale gauge boson is kinematically impossible, the GUT scale baryogenesis does not work well in this scenario.

Recently, it has been pointed out that an inflaton decay will begin in a much more explosive process, called *preheating* [9–14] before the perturbative decay. At this stage, the fluctuation of scalar particles can grow quasi-exponentially by parametric resonance. The importance of this non-perturbative stage was recognized in ref. [9] in the context of the new inflation scenario. As for the chaotic inflation scenario, Kofman, Linde, and Starobinsky first investigated the preheating structure with both massive inflaton and a self-interacting potential [10]. In the case with a self-interacting potential  $\lambda\phi^4/4$  of a massive inflaton, the inflaton particles are produced by parametric resonance due to the self coupling of the inflaton field. In this model, the evolution of inflaton quanta was investigated [11,12] by using a closed time path formalism [15–17] and also studied by fully non-linear lattice simulations [18]. If we adopt the value of  $\lambda \sim 10^{-12}$  which is constrained by density perturbations, it was found that the fluctuation  $\langle\delta\phi^2\rangle \sim 10^{-7}M_{\text{PL}}^2$  will be produced in the preheating stage. In the case of massive inflaton without a self-coupling, however, we do not expect a parametric resonance. Hence one may need another scalar field  $\chi$  coupled to the inflaton field, where coupling makes a resonant production of the  $\chi$ -particle possible. Especially when the coupling constant  $g$  gets large, a parametric resonance will turn on in the broad resonance regime. Consequently, although the expansion of the Universe reduces the amplitude of inflaton field adiabatically, the fluctuation of the  $\chi$  field increases quasi-exponentially. As for the  $\chi$ -particle production, several numerical works have been done by making use of Hartree mean field approximations [19] and fully non-linear calculations [20,21]. Analytic investigations including the backreaction and rescattering effects are performed in ref. [22,23]. Although the structure of resonance shows a complicated feature which is called *stochastic*, the analytic estimations based on the Mathieu equation are found to be reliable to analyze the preheating dynamics.

In the higher-curvature inflation model, a reheating process in the old scenario was considered by Suen and Anderson [24]. In the case of the  $R^2$  inflation model, an effective scalar field that appears by conformal transformation can be

approximately written as a massive scalar field in the reheating phase. Therefore, the preheating stage is absent, since the inflaton fluctuation cannot be amplified by a parametric resonance. In the massive inflaton model, however, a new scenario was recently proposed, in which the non-minimally coupled  $\chi$  field is enhanced by a parametric resonance [25]. Especially when the coupling  $\xi$  is negative, the fluctuation of the  $\chi$ -particle grows rapidly due to negative coupling instability. The final fluctuation  $\langle \chi^2 \rangle \sim 3 \times 10^{-4} M_{\text{PL}}^2$  in the case of  $\xi \approx -4$  is larger than the minimally coupled massive inflaton case with  $g \approx 1 \times 10^{-3}$  [26]. However, in this model, rather large values of  $|\xi|$  are required to have a comparable growth rate with previous existing preheating models. Then a natural question arises. When one considers the non-minimally coupled  $\chi$  field in the context of the higher-curvature inflation model, how is the  $\chi$  fluctuation amplified? If it turns out to be larger as compared with the previous cases, it would affect the baryogenesis in GUT scale [27], a non-thermal phase transition [28] and topological defect formation [29]. We show in this paper that in the higher-curvature inflation model, especially in the  $R^2$  inflation model, significant particle production is expected only due to a non-minimal coupling. As compared with the previous model of chaotic inflation with the non-minimally coupled scalar field  $\chi$ , efficient preheating becomes possible even for rather small  $|\xi|$ .

This paper is organized as follows. In the next section, we briefly review our model of  $R^n$  inflation with the non-minimally coupled scalar field  $\chi$ . In Sec. III, the preheating in the  $R^2$  inflation model is investigated both by analytic approach and numerical integration. We show that analytical estimation based on the Mathieu equation coincides well with numerical results. In Sec. IV, the  $R^4$  inflation case is briefly discussed. We give our conclusions and discussions in the final section.

## II. BASIC EQUATIONS

We propose a model with a higher-curvature term and a non-minimally coupled scalar field  $\chi$ ,

$$\mathcal{L} = \sqrt{-g} \left[ \frac{1}{2\kappa^2} R + \alpha_n R^n - \frac{1}{2} \xi R \chi^2 - \frac{1}{2} (\nabla \chi)^2 - \frac{1}{2} m_\chi^2 \chi^2 \right], \quad (2.1)$$

where  $\kappa^2/8\pi \equiv G = M_{\text{PL}}^{-2}$  is Newton's gravitational constant,  $\alpha_n$  and  $\xi$  are coupling constants, and  $m_\chi$  is a mass of the  $\chi$  field. Although this system contains only one scalar field  $\chi$ , it is reduced to a system described by Einstein-Hilbert action with two scalar fields by making conformal transformation to the Einstein frame [30]. We make the conformal transformation as follows:

$$\hat{g}_{\mu\nu} = e^{2\omega} g_{\mu\nu}, \quad (2.2)$$

where

$$\omega = \frac{\kappa}{\sqrt{6}}\phi \equiv \frac{1}{2}\ln [1 + 2\kappa^2 n \alpha_n R^{n-1} - \xi \kappa^2 \chi^2]. \quad (2.3)$$

Then we obtain the following equivalent Lagrangian:

$$\mathcal{L} = \sqrt{-\hat{g}} \left[ \frac{1}{2\kappa^2} \hat{R} - \frac{1}{2} (\hat{\nabla}\phi)^2 - \frac{1}{2} e^{-\frac{\sqrt{6}}{3}\kappa\phi} (\hat{\nabla}\chi)^2 - U_n(\phi, \chi) \right], \quad (2.4)$$

where the potential  $U_n(\phi, \chi)$  is defined by

$$U_n(\phi, \chi) \equiv e^{-\frac{2\sqrt{6}}{3}\kappa\phi} \left[ \frac{1}{2\kappa^2} R e^{\frac{\sqrt{6}}{3}\kappa\phi} - \frac{1}{2\kappa^2} R - \alpha_n R^n + \frac{1}{2} \xi R \chi^2 + \frac{1}{2} m_\chi^2 \chi^2 \right]. \quad (2.5)$$

Eliminating the Ricci scalar term by using Eq. (2.3),  $U_n(\phi, \chi)$  can be rewritten as

$$U_n(\phi, \chi) = e^{-\frac{2\sqrt{6}}{3}\kappa\phi} \left[ \lambda_n \left( e^{\frac{\sqrt{6}}{3}\kappa\phi} - 1 + \xi \kappa^2 \chi^2 \right)^{\frac{n}{n-1}} + \frac{1}{2} m_\chi^2 \chi^2 \right], \quad (2.6)$$

where

$$\lambda_n \equiv (n-1) \left[ \frac{1}{\alpha_n (2n\kappa^2)^n} \right]^{\frac{1}{n-1}}. \quad (2.7)$$

The scalar field  $\phi$  plays the roll of an inflaton field and the coupling constant  $\alpha_n$  (or  $\lambda_n$ ) is constrained by (i) e-folding by the inflation and (ii) the density perturbation produced in the inflationary stage as follows.

Since we need not take the  $\chi$  field into account in an inflationary stage, the potential  $U_n$  can be approximated as,

$$V_n(\phi) \equiv U_n(\phi, 0) = \lambda_n e^{-\frac{2\sqrt{6}}{3}\kappa\phi} \left( e^{\frac{\sqrt{6}}{3}\kappa\phi} - 1 \right)^{\frac{n}{n-1}}. \quad (2.8)$$

The form of the potential is quite different between the  $n = 2$  case and others. Since the potential has a plateau for  $\phi \gtrsim M_{\text{PL}}$  in the  $n = 2$  case (See Fig. 1), the inflaton rolls down very slowly on this plateau and can give the efficient inflation without making fine tuning on the initial condition of the inflaton field. This is one of the important properties of the  $R^2$  inflation model. In the case of  $n > 2$ , however,  $V_n(\phi)$  has a local maximum at

$$\phi_* = \sqrt{\frac{3}{16\pi}} \log \left[ \frac{2(n-1)}{n-2} \right] M_{\text{PL}}, \quad (2.9)$$

and inflation becomes difficult to realize without fine tuning of the initial value because the inflaton easily falls down to the minimum of the potential. Let us investigate the initial and final value of  $\phi$  in the inflationary stage. First, the slow-roll parameters are described by the potential as

$$\epsilon_1 \equiv \frac{1}{2\kappa^2} \left( \frac{V'_n}{V_n} \right)^2 = \frac{1}{3} \left( 1 - e^{\frac{\sqrt{6}}{3}\kappa\phi} \right)^{-2} \left( 2 - \frac{n-2}{n-1} e^{\frac{\sqrt{6}}{3}\kappa\phi} \right)^2, \quad (2.10)$$

$$\epsilon_2 \equiv \frac{1}{\kappa^2} \frac{V''_n}{V_n} = \frac{2}{3} \left( 1 - e^{\frac{\sqrt{6}}{3}\kappa\phi} \right)^{-2} \left[ 4 - \frac{5n-8}{n-1} e^{\frac{\sqrt{6}}{3}\kappa\phi} + \left( \frac{n-2}{n-1} \right)^2 e^{\frac{2\sqrt{6}}{3}\kappa\phi} \right]. \quad (2.11)$$

The inflationary stage ends when  $\max\{\epsilon_1, |\epsilon_2|\}$  becomes of order unity. One can easily find that  $\epsilon_1$  increases to unity faster than  $|\epsilon_2|$ , and the epoch when inflation ends can be estimated as

$$\phi_f = \sqrt{\frac{3}{16\pi}} \log \left[ \frac{n-1}{2n^2-2n-1} \left\{ (1+\sqrt{3})n+1 \right\} \right] M_{\text{PL}}. \quad (2.12)$$

For example,  $\phi_f = 0.188M_{\text{PL}} \approx M_{\text{PL}}/5$  for  $n=2$ , and  $\phi_f = 0.108M_{\text{PL}} \approx M_{\text{PL}}/9$  for  $n=4$ . Next, let us consider the value of  $\phi$  ( $=\phi_i$ ) at the epoch of horizon exit when physical scales crossed outside the Hubble radius 60 e-folding before the end of inflation. By calculating e-folding number

$$N = -\kappa^2 \int_{\phi_i}^{\phi_e} \frac{V_n}{V'_n} d\phi, \quad (2.13)$$

and setting  $N=60$ , we obtain the value of  $\phi_i$  as

$$\phi_i = \begin{cases} 1.08M_{\text{PL}}, & (n=2) \\ \sqrt{\frac{3}{16\pi}} \log \left[ \frac{2(n-1)}{n-2} - \left\{ \frac{2(n-1)}{n-2} - e^{\frac{\sqrt{6}}{3}\kappa\phi_f} \right\} \left\{ \frac{2(n-1)}{n-2} e^{-\frac{\sqrt{6}}{3}\kappa\phi_f} \right\}^{-\frac{n-2}{n}} e^{-\frac{80(n-2)}{n}} \right] M_{\text{PL}}, & (n \geq 4) \end{cases} \quad (2.14)$$

Note that  $\phi_i$  must be extremely close to the local maximum value  $\phi_*$  for  $n > 2$ .

Next, we calculate the density perturbation produced in the inflationary stage and give the constraint of  $\alpha_n$  by comparing it with COBE data. The amplitude of density perturbation can be calculated as [31]

$$\begin{aligned} \delta_H &= \sqrt{\frac{32}{75} \frac{V_n(\phi_i)}{M_{\text{PL}}^4} \epsilon_1^{-1}(\phi_i)} \\ &= \frac{2\sqrt{2\lambda_n}}{5M_{\text{PL}}^2} e^{-\frac{\sqrt{6}}{3}\kappa\phi_i} \left( e^{\frac{\sqrt{6}}{3}\kappa\phi_i} - 1 \right)^{\frac{3n-2}{2(n-1)}} \left( 1 - \frac{n-2}{2(n-1)} e^{\frac{\sqrt{6}}{3}\kappa\phi_i} \right)^{-1}. \end{aligned} \quad (2.15)$$

The COBE data requires  $\delta_H \lesssim 10^{-5}$ , hence  $\alpha_n$  is constrained to be

$$\begin{cases} \alpha_2 \gtrsim 10^9, & (n=2) \\ \alpha_n = \gamma_n \delta_H^{-2(n-1)} \gtrsim 10^{10(n-1)} \gamma_n, & (n \geq 4) \end{cases} \quad (2.16)$$

where

$$\gamma_n = \frac{M_{\text{PL}}^{2(2-n)}}{(16\pi n)^n} \left\{ \frac{8(n-1)}{25 \left( e^{\frac{\sqrt{6}}{3}\kappa\phi_i} - e^{\frac{\sqrt{6}}{3}\kappa\phi_*} \right)^2} \right\}^{n-1} \left( \frac{n}{n-2} \right)^{3n-2}. \quad (2.17)$$

Note that  $\alpha_n$  needs to take a very large value especially in the  $n \geq 4$  case. This is because the inflation field  $\phi$  must be very near to the local maximum of its potential initially in order to cause the sufficient inflation. For example, in the case of  $n = 4$ , the dimensionless coupling constant  $\beta_4 \equiv \alpha_4 M_{\text{PL}}^4$  is restricted to be

$$\beta_4 \gtrsim 10^{126}. \quad (2.18)$$

As the increase of  $n$ , we have to choose larger values of the coupling constant to fit the COBE data. However, since we are interested in preheating after inflation, it is worth investigating how  $\chi$ -particles are amplified apart from the constraint of the coupling constant even for the  $n \geq 4$  case.

After the inflationary stage ended, the universe enters the oscillating phase of the  $\phi$  field and  $\chi$ -particles can be created because the  $\chi$  field is non-minimally coupled with the spacetime curvature which is oscillated by the  $\phi$  field. Let us obtain the basic equations of the  $R^n$  inflation model in the preheating stage. Since the  $\chi$  field is treated as a quantum field on the classical background of spacetime and the  $\phi$  field, the conformal factor in Eq. (2.2) includes a quantum variable. However, in order not to discuss quantum gravity, this term should be replaced with an expectation value  $\langle \chi^2 \rangle$ , which may correspond to the number density of the  $\chi$ -particle. Then we regard the conformal factor  $\Omega^2$  as  $1 - \eta$ , where  $\eta \equiv \xi \kappa^2 \langle \chi^2 \rangle$  [32].

Since we assume that the spacetime and the inflaton field are spatially homogeneous, we adopt the flat Friedmann-Robertson-Walker metric as the background spacetime;

$$d\hat{s}^2 = -dt^2 + \hat{a}^2(t) d\mathbf{x}^2. \quad (2.19)$$

Hereafter we drop a caret since we argue only in the Einstein frame. From the Lagrangian (2.4), the evolution of the scale factor is described by

$$\left( \frac{\dot{a}}{a} \right)^2 = \frac{\kappa^2}{3} \left[ \frac{1}{2} \dot{\phi}^2 + \frac{1}{2} e^{-\frac{\sqrt{6}}{3} \kappa \phi} \langle (\nabla \chi)^2 \rangle e^{-\frac{2\sqrt{6}}{3} \kappa \phi} \left\{ \lambda_n \left( e^{\frac{\sqrt{6}}{3} \kappa \phi} - 1 + \eta \right)^{\frac{n}{n-1}} + \frac{1}{2} m_\chi^2 \langle \chi^2 \rangle \right\} \right], \quad (2.20)$$

where a dot denotes a derivative with respect to time coordinate  $t$ .

The evolution of the homogeneous inflaton field  $\phi$  yields

$$\begin{aligned} \ddot{\phi} + \frac{3\dot{a}}{a} \dot{\phi} - \frac{2\sqrt{6}}{3} \kappa e^{-\frac{2\sqrt{6}}{3} \kappa \phi} \left[ \frac{1}{4} e^{\frac{\sqrt{6}}{3} \kappa \phi} \langle (\nabla \chi)^2 \rangle \right. \\ \left. + \lambda_n \left( e^{\frac{\sqrt{6}}{3} \kappa \phi} - 1 + \eta \right)^{\frac{1}{n-1}} \left\{ \frac{n-2}{2(n-1)} e^{\frac{\sqrt{6}}{3} \kappa \phi} - 1 + \eta \right\} + \frac{1}{2} m_\chi^2 \langle \chi^2 \rangle \right] = 0. \end{aligned} \quad (2.21)$$

Since we postulate that the  $\phi$  field is spatially homogeneous, the fluctuation  $\delta\phi$  is not considered. In the present model, the  $\phi$  field is a product of purely gravitational origin. Hence considering the fluctuation  $\delta\phi$  is equivalent to

taking into account the perturbation of the metric. Recently, Bassett et al. [39] investigated the evolution of metric perturbation in a two-field model of a massive inflaton and a massless  $\chi$  field interacting with the inflaton, and found that metric fluctuation is resonantly amplified in preheating phase. There will be a possibility that  $\delta\phi$  grows by a parametric resonance also in the present model. Moreover, the rescattering effect of the  $\chi$ -particle and the  $\delta\phi$  field are expected to make the  $\chi$  field be amplified. Although we do not consider the  $\phi$  fluctuation in this paper, we should take into account this effect for a complete study of preheating. It is under consideration.

The equation of the  $\chi$  field is expressed as

$$\ddot{\chi} + \left( \frac{3\dot{a}}{a} - \frac{\sqrt{6}}{3}\kappa\dot{\phi} \right) \dot{\chi} - \partial_i \partial^i \chi + e^{-\frac{\sqrt{6}}{3}\kappa\phi} \frac{\partial}{\partial \chi} \left[ \lambda_n \left( e^{\frac{\sqrt{6}}{3}\kappa\phi} - 1 + \xi \kappa^2 \chi^2 \right)^{\frac{n}{n-1}} + \frac{1}{2} m_\chi^2 \chi^2 \right] = 0, \quad (2.22)$$

where an index with a roman character denotes space coordinates. In order to study a quantum particle creation of the  $\chi$  field, we make the following mean field approximation with respect to  $\chi$ , which provides us a linearized equation for the quantum field  $\chi$ :

$$\ddot{\chi} + \left( \frac{3\dot{a}}{a} - \frac{\sqrt{6}}{3}\kappa\dot{\phi} \right) \dot{\chi} - \partial_i \partial^i \chi + e^{-\frac{\sqrt{6}}{3}\kappa\phi} \nabla_\chi^2 \left[ \lambda_n \left( e^{\frac{\sqrt{6}}{3}\kappa\phi} - 1 + \eta \right)^{\frac{n}{n-1}} + \frac{1}{2} m_\chi^2 \langle \chi^2 \rangle \right] \chi = 0. \quad (2.23)$$

where  $\nabla_\chi = 2\sqrt{\langle \chi^2 \rangle} \partial/\partial \langle \chi^2 \rangle$ . Expanding the scalar field  $\chi$  as

$$\chi = \frac{1}{(2\pi)^{3/2}} \int \left( a_k \chi_k(t) e^{-i\mathbf{k}\cdot\mathbf{x}} + a_k^\dagger \chi_k^*(t) e^{i\mathbf{k}\cdot\mathbf{x}} \right) d^3\mathbf{k}, \quad (2.24)$$

where  $a_k$  and  $a_k^\dagger$  are the annihilation and creation operators, respectively,  $\chi_k$  obeys the following equation of motion:

$$\begin{aligned} \ddot{\chi}_k + \left( \frac{3\dot{a}}{a} - \frac{\sqrt{6}}{3}\kappa\dot{\phi} \right) \dot{\chi}_k + \left[ \frac{k^2}{a^2} + e^{-\frac{\sqrt{6}}{3}\kappa\phi} \right. \\ \left. \times \left\{ \frac{2n}{n-1} \lambda_n \xi \kappa^2 \left( e^{\frac{\sqrt{6}}{3}\kappa\phi} - 1 + \eta \right)^{-\frac{n-2}{n-1}} \left( e^{\frac{\sqrt{6}}{3}\kappa\phi} - 1 + \frac{n+1}{n-1} \eta \right) + m_\chi^2 \right\} \right] \chi_k = 0. \end{aligned} \quad (2.25)$$

The expectation value of  $\chi^2$  is expressed with  $\chi_k$  as

$$\langle \chi^2 \rangle = \frac{1}{2\pi^2} \int k^2 |\chi_k|^2 dk. \quad (2.26)$$

Let us obtain the approximate equations of the  $\phi$  and  $\chi$  fields in order to estimate the preheating phenomenon analytically. First we rewrite Eqs. (2.20) and (2.21) by following two approximations:

1. The value of  $\phi$  is much smaller than  $M_{\text{PL}}$ , namely

$$\phi \ll M_{\text{PL}}. \quad (2.27)$$

2. The backreaction effect by the  $\chi$ -particles is negligible, namely

$$\eta \ll 1 \quad \text{and} \quad \langle (\nabla \chi)^2 \rangle \ll M_{\text{PL}}^4. \quad (2.28)$$

Then, the evolution equation of the scale factor (2.20) is written by

$$\left(\frac{\dot{a}}{a}\right)^2 = \frac{\kappa^2}{3} \left[ \frac{1}{2} \dot{\phi}^2 + K_n \phi^{\frac{n}{n-1}} \right], \quad (2.29)$$

where

$$K_n \equiv \lambda_n \left( \frac{2}{3} \kappa^2 \right)^{\frac{n}{2(n-1)}}, \quad (2.30)$$

is a constant. On the other hand, the  $\phi$  field equation (2.21) can be written by

$$\ddot{\phi} + \frac{3\dot{a}}{a} \dot{\phi} + \frac{n}{n-1} K_n \phi^{\frac{1}{n-1}} = 0. \quad (2.31)$$

Note that the potential of the  $\phi$  field in reheating phase is represented as  $V_n(\phi) \approx K_n \phi^{\frac{n}{n-1}}$ . For  $n = 2$ , the potential becomes  $V_2(\phi) \approx K_2 \phi^2$ , and the  $\phi$  field behaves as a massive inflaton. For  $n \geq 4$ , the potential is not regarded as the mass term and the curvature of the potential around its bottom becomes larger than that in the  $n = 2$  case (See Fig 1).

Making use of a time averaged relation:  $\langle \dot{\phi}^2 \rangle = \frac{n}{n-1} \langle V_n(\phi) \rangle$ , we can easily find the time evolution of the scale factor from the relations (2.29) and (2.31) as

$$a \approx \left( \frac{t}{t_0} \right)^{\frac{3n-2}{3n}}, \quad (2.32)$$

where  $t_0$  is the initial time of the coherent oscillation. Then, introducing a new time variable

$$\tau \equiv \frac{n}{2(n-1)} t_0 \left( \frac{t}{t_0} \right)^{\frac{2(n-1)}{n}} = \frac{n}{2(n-1)} t_0 a^{\frac{6(n-1)}{3n-2}}, \quad (2.33)$$

and a new scalar field

$$\varphi \equiv \left( \frac{t}{t_0} \right)^{\frac{2(n-1)}{n}} \phi = a^{\frac{6(n-1)}{3n-2}} \phi, \quad (2.34)$$

the  $\phi$  field equation (2.31) is rewritten as

$$\frac{d^2 \varphi}{d\tau^2} + \frac{n}{n-1} K_n \varphi^{\frac{1}{n-1}} = 0. \quad (2.35)$$

This equation is easy to be integrated and we find a conserved quantity,



$$E \equiv \frac{1}{2} \left( \frac{d\varphi}{d\tau} \right)^2 + K_n \varphi^{\frac{n}{n-1}}. \quad (2.36)$$

Integrating Eq. (2.36) by the variable  $\zeta \equiv \left( \frac{K_n}{E} \right)^{\frac{1}{n}} \varphi^{\frac{1}{n-1}}$ ,  $\tau$  is represented as

$$\tau = \pm \frac{n-1}{\sqrt{2E}} \left( \frac{E}{K_n} \right)^{\frac{n-1}{n}} \int \frac{\zeta^{n-2}}{\sqrt{1-\zeta^n}} d\zeta. \quad (2.37)$$

For example, when  $n = 2$ ,  $\tau$  is written as  $\tau = (1/\sqrt{2K_2}) \cos^{-1} \zeta + \tau_0$ . Hence the oscillation of the  $\varphi$  field is sinusoidal:

$$\varphi = \sqrt{\frac{E}{K_2}} \cos \left[ \sqrt{2K_2}(\tau - \tau_0) \right]. \quad (2.38)$$

For  $n > 2$ , however, the  $\varphi$  field does not oscillate sinusoidally but its behavior is rather complicated since the integral in Eq (2.37) is expressed by an elliptic or hyperelliptic integral. We investigate this issue for the  $n = 4$  case in Sec. IV.

Next we rewrite the  $\chi$  field equation (2.25) with the new time variable  $\tau$ . It yields

$$\begin{aligned} & \frac{d^2 \chi_k}{d\tau^2} + 2b \frac{d\chi_k}{d\tau} + a^{-\frac{6(n-2)}{3n-2}} \left[ \frac{k^2}{a^2} + e^{-\frac{\sqrt{6}}{3}\kappa\phi} \right. \\ & \times \left. \left\{ \frac{2n}{n-1} \lambda_n \xi \kappa^2 \left( e^{\frac{\sqrt{6}}{3}\kappa\phi} - 1 + \eta \right)^{-\frac{n-2}{n-1}} \left( e^{\frac{\sqrt{6}}{3}\kappa\phi} - 1 + \frac{n+1}{n-1} \eta \right) + m_\chi^2 \right\} \right] \chi_k = 0, \end{aligned} \quad (2.39)$$

where

$$b \equiv \frac{6(n-1)}{3n-2} \frac{1}{a} \frac{da}{d\tau} - \frac{\kappa}{\sqrt{6}} \frac{d\phi}{d\tau}. \quad (2.40)$$

Transforming the scalar field  $\chi_k$  as

$$X_k \equiv e^{\int b d\tau} \chi_k = a^{\frac{6(n-1)}{3n-2}} e^{-\frac{\kappa}{\sqrt{6}}\kappa\phi} \chi_k, \quad (2.41)$$

Eq. (2.39) becomes

$$\frac{d^2 X_k}{d\tau^2} + \omega_k^2 X_k = 0, \quad (2.42)$$

where the time dependent frequency  $\omega_k^2$  is

$$\begin{aligned} \omega_k^2 \equiv & a^{-\frac{6(n-2)}{3n-2}} \left[ \frac{k^2}{a^2} + e^{-\frac{\sqrt{6}}{3}\kappa\phi} \left\{ \frac{2n}{n-1} \lambda_n \xi \kappa^2 \left( e^{\frac{\sqrt{6}}{3}\kappa\phi} - 1 + \eta \right)^{-\frac{n-2}{n-1}} \left( e^{\frac{\sqrt{6}}{3}\kappa\phi} - 1 + \frac{n+1}{n-1} \eta \right) + m_\chi^2 \right\} \right] \\ & - \frac{6(n-1)}{3n-2} \left\{ \frac{1}{a} \left( \frac{d^2 a}{d\tau^2} \right) - \frac{1}{a^2} \left( \frac{da}{d\tau} \right)^2 \right\} + \frac{\kappa}{\sqrt{6}} \frac{d^2 \phi}{d\tau^2} - \left\{ \frac{6(n-1)}{3n-2} \frac{1}{a} \frac{da}{d\tau} - \frac{\kappa}{\sqrt{6}} \frac{d\phi}{d\tau} \right\}^2. \end{aligned} \quad (2.43)$$

Since the frequency of the  $X_k$  field includes the inflaton field which oscillates coherently under two approximations (2.27) and (2.28), the parametric resonance may be expected due to these terms even in the  $n \geq 4$  case. We

investigate  $\chi$ -particle production by the oscillating background field  $\phi$  especially when  $n = 2$  and  $n = 4$ . We follow the semiclassical picture of preheating which is first considered in Ref. [18], where the  $\chi$ -particles are created by quantum fluctuation initially, and they are treated as a classical field later as the  $\chi$ -particles are produced. We give an initial distribution of  $X_k$ -state in our previous paper [26]. In the next section, we analyze the structure of preheating for the  $n = 2$  case and compare it with numerical results.

### III. PREHEATING BY $R^2$ INFLATION MODEL

In the  $n = 2$  case, the reheating phase starts at  $\phi \approx M_{\text{PL}}/5$  and the  $\phi$  field begins to oscillate coherently around the minimum of its potential after  $\phi$  drops down to  $\phi \lesssim M_{\text{PL}}/20$ . At this stage, as is found from Eqs. (2.32)-(2.34), the scale factor evolves as  $a \approx (t/t_0)^{2/3}$  and  $\tau, \varphi$  are defined by  $\tau = t$  and  $\varphi = a^{3/2}\phi$ . Since the  $\varphi$  field oscillates sinusoidally as Eq. (2.38) with the mass

$$m \equiv \sqrt{2K_2} = \frac{M_{\text{PL}}}{\sqrt{96\pi\alpha_2}}, \quad (3.1)$$

the evolution of the  $\phi$  field for  $\phi \lesssim M_{\text{PL}}/20$  is sinusoidal with decreasing amplitude  $\Phi$  [22]:

$$\phi = \Phi \sin mt, \quad \text{with} \quad \Phi = \frac{M_{\text{PL}}}{\sqrt{3\pi}mt} = \frac{M_{\text{PL}}}{2\pi\sqrt{3\pi}\bar{t}}, \quad (3.2)$$

which is equivalent to the case of the massive inflaton. Here we introduced the dimensionless time variable  $\bar{t} \equiv mt/2\pi$ , which represents the number of the oscillation of the inflaton field. Note that Eq. (3.2) is valid for  $\bar{t} \gtrsim 1$ . As the  $\chi$ -particles are produced, the backreaction effect by  $\eta$  and  $\langle(\nabla\chi)^2\rangle$  is expected to appear. However, numerical calculations shows that  $\eta$  and  $\langle(\nabla\chi)^2\rangle/m^2M_{\text{PL}}^2$  do not exceed 0.1 even at the final stage of preheating, and the  $\varphi$  field oscillates almost coherently during the whole stage of preheating.

Let us investigate the evolution of  $\langle\chi^2\rangle$  both analytically and numerically. First,  $\langle\chi^2\rangle$  is normalized as

$$\langle\bar{\chi}^2\rangle \equiv \frac{\langle\chi^2\rangle}{M_{\text{PL}}^2} = \left(\frac{m}{M_{\text{PL}}}\right)^2 \frac{1}{2\pi^2} \int \bar{k}^2 |\bar{\chi}_k|^2 d\bar{k} = \frac{1}{96\pi\alpha_2} \frac{1}{2\pi^2} \int \bar{k}^2 |\bar{\chi}_k|^2 d\bar{k}, \quad (3.3)$$

where  $\bar{k} = k/m$  and  $\bar{\chi}_k = \sqrt{m}\chi_k$ . Hence  $\langle\bar{\chi}^2\rangle$  depends on the coupling constant  $\alpha_2$ . Here we adopt the lowest value  $\alpha_2 = 2 \times 10^9$  which is determined by density perturbation. Note that in this case,  $m \sim 10^{-6}M_{\text{PL}} \sim 10^{13}$  GeV, which is almost the same value as that in the chaotic inflation model. Next, let us rewrite Eq. (2.42) to the form of Mathieu equation. Since the scale factor decreases so slow as compared with the time scale of the oscillation of the inflaton field for  $\phi \lesssim M_{\text{PL}}/20$ , we can approximate the frequency as

$$\begin{aligned}\omega_k^2 &\approx \frac{k^2}{a^2} + 4\lambda_2 \xi \kappa^2 \left\{ 1 - (1 - 3\eta) \left( 1 - \frac{\sqrt{6}}{3} \kappa \phi \right) \right\} + m_\chi^2 \left( 1 - \frac{\sqrt{6}}{3} \kappa \phi \right) + \frac{\kappa}{\sqrt{6}} \frac{d^2 \phi}{d\tau^2} \\ &\approx \frac{k^2}{a^2} + m_\chi^2 + 9\xi\eta m^2 + \frac{2}{3\pi\bar{t}} \left[ 3\xi m^2(1 - 3\eta) - m_\chi^2 - \frac{1}{2}m^2 \right] \sin mt.\end{aligned}\quad (3.4)$$

Here we did not neglect  $\eta$ . Since  $\eta$  may increase up to 0.1, we should consider the effect from the backreaction terms  $\xi\eta$  and  $3\eta$  in the  $X_k$  field equation. Setting  $mt = 2z - \pi/2$ , Eq. (2.42) is reduced to the Mathieu equation:

$$\frac{d^2}{dz^2} X_k + (A_k - 2q \cos 2z) X_k = 0, \quad (3.5)$$

where

$$A_k = 4 \left( \frac{\bar{k}^2}{a^2} + \bar{m}_\chi^2 + 9\xi\eta \right), \quad (3.6)$$

$$q = \frac{4}{3\pi\bar{t}} \left[ 3\xi(1 - 3\eta) - \bar{m}_\chi^2 - \frac{1}{2} \right]. \quad (3.7)$$

$\bar{m}_\chi$  is normalized as  $\bar{m}_\chi = m_\chi/m$ . Since we can find from Eq. (3.6) that  $A_k$  always takes positive value even in the negative  $\xi$  case [Remember  $\eta = \xi\kappa^2\langle\chi^2\rangle$ ], the resonance bands are narrower than those in the model discussed in Ref. [26] when  $\xi < 0$  case. However, since  $A_k$  is not limited by  $A_k \geq 2q$ , the resonance bands can be broader than those in the model of  $\frac{1}{2}m^2\phi^2 + \frac{1}{2}g^2\phi^2\chi^2$ . Moreover  $q$  decreases as  $1/\bar{t}$  by the expansion of the universe. This is slower than in the massive inflaton plus coupled scalar field case, where  $q \sim 1/\bar{t}^2$  [26]. This is due to the fact that the dominant oscillating term in Eq. (3.4) is not the  $\phi^2$  term but the  $\phi$  term, hence the period of the preheating becomes rather longer and we can expect an efficient resonance even if  $|\xi|$  is not very large. Below, we consider the case of  $\xi > 0$  and  $\xi < 0$  separately.

### A. Case of $\xi \geq 0$

#### 1. massless $\chi$ -particle case

First, we investigate the production of the massless  $\chi$ -particle for the case  $\xi > 0$ . In the initial stage of preheating, we can neglect the  $\xi\eta$  term. Hence  $A_k$  is almost constant ( $A_k \approx 0$ ) if we consider modes with small momentum  $\bar{k}$ , which may be the dominant ingredients of the particle production independently on  $\xi$ . When the  $\phi$  field begins to oscillate coherently ( $\bar{t} \approx 1$ ), i.e., the analysis by using the Mathieu equation becomes valid, the initial value of  $q$  ( $= q_i$ ) is determined by  $\xi$ . After this,  $q$  decreases as  $1/\bar{t}$  by the expansion of the universe. Hence the Mathieu parameters trace the line near the  $q$ -axis horizontally on the Mathieu chart. When the  $\chi$  field passes across the first instability

band, the resonance terminates. What determines the efficiency of the preheating is the initial value of  $q$ . When  $q_i$  is large, the Floquet index is large and the growth rate of  $\langle \bar{\chi}^2 \rangle$  is expected to be large. Moreover the period when the Mathieu parameters stay in the instability band becomes long, which means that the total abundance of  $\langle \bar{\chi}^2 \rangle$  may be large. As a result, we can conclude that the large  $\xi$  gives the efficient preheating as long as the backreaction effect can be neglected. Let us examine the evolution with the concrete values of  $\xi$  numerically.

For small  $\xi$  ( $\xi \lesssim 1$ ),  $q_i \lesssim 1$ . Hence, parametric resonance turns on in the narrow resonance regime and  $\chi$ -particles are hardly produced because  $q$  decreases and the resonant range becomes narrower and narrower by the expansion of the universe. On the other hand, for  $\xi \gtrsim 1$ , the resonance can be expected. Let us consider several cases to compare the differences of the resonance structures. For  $\xi = 3$ ,  $q_i \sim 3.61$ , and the resonance band is rather broad at the initial stage. In Fig. 3(a), we depict the evolution of  $\langle \bar{\chi}^2 \rangle \equiv \langle \chi^2 \rangle / M_{\text{PL}}^2$  as a function of  $\bar{t}$  for  $\xi = 3$ . After  $\bar{t} \approx 1$ ,  $\langle \bar{\chi}^2 \rangle$  increases almost exponentially by the parametric resonance, and it reaches its maximum value  $\langle \bar{\chi}^2 \rangle_f = 2.21 \times 10^{-8}$  when  $\bar{t}_f = 5.61$ . [We summarize the data of numerical calculations in Table I.] After that,  $\langle \bar{\chi}^2 \rangle$  decreases monotonically by the adiabatic damping of the Hubble expansion. Since the total amount of created particles is not so large,  $\xi\eta$  is much smaller than unity during the whole stage and we can neglect the backreaction effect. In this case, the factor which terminates the resonance is the expansion of the universe.  $A_k$  and  $q$  both decrease and the resonance stops when  $q$  drops down to  $q_f = 0.64$  ( $\bar{t}_f = 5.61$ ). This evolution is illustrated by the solid curve in Fig. 2. For  $\xi = 5$ ,  $q_i \sim 6.15$ , and more efficient resonance can occur. Actually, the final value of  $\langle \bar{\chi}^2 \rangle_f = 1.74 \times 10^{-4}$  (when  $\bar{t}_f = 6.27$  and  $q_f = 0.98$ ) is much larger than the case of  $\xi = 3$  (Fig. 3(b)). Since the term  $36\xi\eta$  in Eq. (3.6) is about 3.94 at  $\bar{t}_f = 6.27$ . Hence we can not neglect the backreaction in this case. The backreaction mainly affects the behavior of  $A_k$ . It makes  $A_k$  increase rapidly independently on the momentum  $k$ . Hence the Mathieu parameter deviates from the first instability band and the resonant band becomes very narrow. By this effect the parametric resonance terminates. For  $\xi = 5$ , however, this deviation occurs when  $q$  drops down to about unity, hence we can say that the final value of  $\langle \bar{\chi}^2 \rangle$  is mainly determined by the decrease of  $q$ . The case of  $\xi \approx 5$  is the marginal case, whether the value of  $\langle \bar{\chi}^2 \rangle_f$  is determined by the decrease of  $q$  due to the expansion of the universe, or by the increase of  $A_k$  due to the backreaction.

We can find that  $\langle \bar{\chi}^2 \rangle$  increases with the same period as the oscillation of the inflaton field. This is different from the resonance in the chaotic inflation model with the massive inflation, where the  $\langle \bar{\chi}^2 \rangle$  increases twice during one oscillation of the inflation [22]. In the chaotic inflation model, the Mathieu parameters are constrained as  $A_k \geq 2q$ ,

and the square of the time dependent frequency of the  $\chi$  field is always positive. And the resonance occurs when the non-adiabatic condition:  $\omega_k^2 \ll d\omega_k/dt$  is satisfied. Since this condition is realized when  $\phi \approx 0$ , the resonance occurs twice during each oscillation of the inflaton field. In the present case, however,  $\omega_k^2$  is not constrained to be positive but can become a negative value. In this case  $\chi$ -particles are produced mainly by negative coupling instability [25]. As we can see from Eq (3.4),  $\omega_k^2$  becomes negative once for each oscillation of  $\phi$ . As a result,  $\langle \bar{\chi}^2 \rangle$  increases once during each oscillation of the  $\phi$  field. This picture is independent on the sign of the coupling constant  $\xi$ .

For  $\xi = 10$ ,  $q_i \sim 12.52$ , and the final values are  $t_f = 4.28$ ,  $q_f = 2.71$ , and  $\langle \bar{\chi}^2 \rangle_f = 9.95 \times 10^{-5}$  (Fig. 3(c)). In this case, the value of  $\langle \bar{\chi}^2 \rangle_f$  decreases slightly compared with the  $\xi = 5$  case. As the  $\chi$ -particles are created,  $A_k$  increases because of the  $\xi\eta$  term and the  $\chi$  field deviates from instability bands before  $q$  drops down under unity. This behavior is illustrated by the dashed curve in Fig. 2. Namely, in this case, the created  $\chi$ -particles themselves terminate the resonance. For  $\xi \gtrsim 5$ , the mechanism to stop the resonance is the same as in the  $\xi = 10$  case. One can estimate the final abundance  $\langle \bar{\chi}^2 \rangle_f$  by making use of this property. The maximal momentum to cause the negative coupling instability is given by Eq (3.4) as

$$\frac{\bar{k}_{max}^2}{a^2} = \frac{2}{3\pi\bar{t}} \left[ 3\xi(1-3\eta) - m_\chi^2 - \frac{1}{2} \right] - 9\xi\eta - \bar{m}_\chi^2, \quad (3.8)$$

where  $\bar{k}_{max} \equiv k_{max}/m$  and  $\bar{m}_\chi \equiv m_\chi/m$ . The relation (3.8) suggests that  $\bar{k}_{max}^2/a^2$  decreases and approaches zero as the preheating proceeds. Actually, numerical calculation shows that  $\bar{k}_{max}^2/a^2$  reaches zero at  $\bar{t}_f$  in the case of  $\xi \gtrsim 5$ . For this reason, it is enough to set  $\bar{k}^2/a^2 = 0$  in Eq. (3.6) in order to obtain the analytical value of  $\langle \bar{\chi}^2 \rangle_f$ . For  $\xi \gtrsim 5$ , parametric resonance terminates when  $A_k$  begins to increase rapidly as the increase of  $\xi\eta$ . Since the resonance bands are very narrow for the region  $A_k \gtrsim 3q$ , we adopt the criterion: When the Mathieu parameters pass across the  $A_k = 3q$  line, the preheating terminates. Then, we find the final abundance of the  $\chi$ -particles as

$$\langle \bar{\chi}^2 \rangle_f \approx \frac{1}{24\pi\xi(\pi\bar{t}_f + 1)} \left( 1 - \frac{1}{6\xi} \right). \quad (3.9)$$

Note that  $\langle \bar{\chi}^2 \rangle_f$  includes two variables:  $\xi$  and  $\bar{t}_f$ . Generally, as  $\xi$  increases ( $\xi \gtrsim 5$ ),  $\bar{t}_f$  decreases because the production rate of  $\chi$ -particles becomes large and the  $\chi$  field deviates from the instability bands in the early stage. Numerically,  $\langle \bar{\chi}^2 \rangle_f$  is the slowly decreasing function of  $\xi$  for  $\xi \gtrsim 5$  and this suggests that the  $\xi$  effect plays a more important role. The analytic estimation by Eq. (3.9) shows good agreement with numerical calculation. For example, when  $\xi = 10$ , the estimated value is  $\langle \bar{\chi}^2 \rangle_f = 9.02 \times 10^{-5}$  and the numerical value is  $\langle \bar{\chi}^2 \rangle_f = 9.95 \times 10^{-5}$ . For  $\xi = 100$ , the analytic value is  $\langle \bar{\chi}^2 \rangle_f = 2.87 \times 10^{-5}$ , since  $\bar{t}_f = 1.15$ . This is close to the numerical value  $\langle \bar{\chi}^2 \rangle_f = 2.51 \times 10^{-5}$ .

This coincidence shows the validity of the criterion and the picture which we adopted. For  $\xi \gtrsim 100$ ,  $\bar{t}_f$  approaches a constant value  $\bar{t}_f \sim 1$ , and  $\langle \bar{\chi}^2 \rangle_f$  decreases as  $1/\xi$ . Other examples are listed in Table I. We also show the final value of  $\langle \bar{\chi}^2 \rangle_f$  as a function of  $\xi$  in Fig. 4. For  $1 \lesssim \xi \lesssim 5$ ,  $\langle \bar{\chi}^2 \rangle_f$  is the increasing function of  $\xi$  and is determined by the decrease of  $q$  due to the Hubble expansion. On the other hand,  $\langle \bar{\chi}^2 \rangle_f$  is a slowly decreasing function of  $\xi$  for  $\xi \gtrsim 5$ , where the backreaction effect becomes important.

We can conclude that  $\langle \bar{\chi}^2 \rangle_f$  takes maximal value  $\langle \bar{\chi}^2 \rangle_{max} = 1.74 \times 10^{-4}$  when  $\xi \approx 5$  for  $\xi > 0$  for the massless  $\chi$ -particle case.

## 2. massive $\chi$ -particle case

Whether the  $\chi$ -particle with a mass heavier than the GUT scale can be produced or not is one of the most important issues of the preheating, which is related to GUT scale baryogenesis. One can easily obtain the properties of the preheating by the massive  $\chi$  field and difference from the massless case from Eqs. (3.6) and Eq. (3.7). Since the  $\chi$ -field couples with the inflaton field by  $\xi$  and  $m_\chi$  terms as we can see from Eq. (2.25), one may consider that parametric resonance would occur by only the mass term without the non-minimal coupling. This, however, is not the case. In the case of  $\xi = 0$ ,  $A_k \geq 4\bar{m}_\chi^2$  and  $|q_i| \approx 0.4(\bar{m}_\chi^2 + \frac{1}{2})$ . This means that  $A_k$  is at least 10 times larger than  $q$  when  $\bar{t} \approx 1$ , in which case the resonance bands are very narrow. Moreover, even if the  $\chi$  field stays in an instability band initially,  $A_k$  and  $q$  decrease by the expansion of the universe and soon deviate from the instability bands. As a result, it is difficult to produce the massive  $\chi$ -particle enough without the non-minimal coupling. We confirmed this by numerical calculation.

For the  $m_\chi \neq 0$  case, the existence of the  $\bar{m}_\chi^2$  term constrains  $A_k \geq 4\bar{m}_\chi^2$  and decreases the value of  $q$ , hence the resonance is suppressed as compared with the massless case. First, consider the case of  $m_\chi = m$  ( $\bar{m}_\chi = 1$ ).  $A_k$  takes the value more than 4 due to the mass effect, and the modes with the momentum which contribute to the resonance mainly exist in the second instability band of the Mathieu chart (See Fig. 2). Since there is no contribution from the first resonance band, which has larger Floquet index than the second one with the same  $q$  value, the larger value of  $\xi$  is expected to be needed for the  $\chi$ -particle production to occur. Numerically, when  $\xi \lesssim 3$ , the parametric resonance does not come about. In the case of  $\xi = 5$ , the resonance occurs, but this process is very weak (Fig. 5(a)). For  $\bar{t} \gtrsim 1$ ,  $\langle \bar{\chi}^2 \rangle$  increases, but  $\langle \bar{\chi}^2 \rangle_f$  is smaller than the initial value. When  $\xi = 10$ , the parametric resonance after  $\bar{t} \approx 1$  is rather effective (Fig. 5(b)). The final values are  $\bar{t}_f = 9.22$ ,  $q_f = 1.31$ , and  $\langle \bar{\chi}^2 \rangle_f = 1.17 \times 10^{-5}$  (See Table II).

Since the contribution from the backreaction term  $36\xi\eta$  in Eq. (3.6) takes 1.06 as a final value, the deviation from the instability band by the increase of  $A_k$  begins to be important. When  $\xi = 20$ , the final values are  $\bar{t}_f = 3.23$ ,  $q_f = 7.07$ , and  $\langle\bar{\chi}^2\rangle_f = 5.19 \times 10^{-5}$  (Fig. 5(c)). In this case, the backreaction effect by the  $\xi\eta$  term completely determines the final  $\chi$ -particle abundance because  $q_f = 7.07$  when resonance ends. Numerically,  $\langle\bar{\chi}^2\rangle_f$  takes the maximal value of  $\langle\bar{\chi}^2\rangle_{max} \approx 5 \times 10^{-5}$  for  $\xi = 20 \sim 30$ . For  $\xi \gtrsim 30$ ,  $\langle\bar{\chi}^2\rangle_f$  is a slowly decreasing function of  $\xi$ . Generally, when the  $\xi\eta$  suppression effect plays the relevant role, one can estimate  $\langle\bar{\chi}^2\rangle_f$  in the same way as the massless  $\chi$ -particle case. By adopting the criterion:  $A_k = 3q$  when the resonance terminates and setting  $\bar{k}^2/a^2 = 0$  in Eq. (3.6), we obtain

$$\langle\bar{\chi}^2\rangle_f \approx \frac{1}{72\pi\xi^2} \left[ \frac{6\xi - 1}{2(\pi\bar{t}_f + 1)} - \bar{m}_\chi^2 \right]. \quad (3.10)$$

Apparently, the mass effect suppresses the final  $\chi$ -particle abundance. Let us compare this estimation with numerical results. For example, when  $\bar{m}_\chi = 1$  and  $\xi = 20$ , the numerical value is  $\langle\bar{\chi}^2\rangle_f = 5.19 \times 10^{-5}$  (at  $\bar{t}_f = 3.23$ ) and the analytic one is  $\langle\bar{\chi}^2\rangle_f = 4.80 \times 10^{-5}$ ; for  $\xi = 100$ , the numerical one is  $\langle\bar{\chi}^2\rangle_f = 2.78 \times 10^{-5}$  (at  $\bar{t}_f = 1.18$ ) and the analytic one is  $\langle\bar{\chi}^2\rangle_f = 2.76 \times 10^{-5}$ . When  $\bar{m}_\chi = 1$ , the mass term in Eq. (3.10) can not be neglected as compared with the former term for the  $\xi \lesssim 50$  case. In this case, the mass effect is one of the important factors to determine the final abundance of the  $\chi$  particles. On the other hand, for  $\xi \gtrsim 50$ , the mass effect can be neglected and does not play a relevant role for the final abundance, although the growth rate and other properties during the resonance are different from the massless case. In Table II, we show the analytically estimated and numerical values of  $\langle\bar{\chi}^2\rangle_f$  in various parameters. We can see that the analytic results give good agreement with the numerical ones.

For the large  $\xi$  where the backreaction becomes important, the right hand side (r.h.s.) in Eq. (3.10) must be a positive value, hence  $\bar{m}_\chi$  is constrained to be

$$\bar{m}_\chi^2 \lesssim \frac{6\xi - 1}{2(\pi\bar{t}_f + 1)}. \quad (3.11)$$

Since  $\bar{t}_f$  approaches to the constant value of  $\bar{t}_f \approx 1$  as  $\xi$  increases, we can obtain the constraint of the mass of the created  $\chi$ -particle for large  $\xi$  as

$$\bar{m}_\chi \lesssim \sqrt{\xi}. \quad (3.12)$$

From this constraint we find that if  $\xi$  is more than 100,  $\chi$ -particle whose mass is of order  $m_\chi = 10m \sim 10^{14}$  GeV can be produced by the non-minimal coupling in the  $R^2$  inflation model. In order to produce the GUT scale gauge boson whose mass is about  $m_\chi = 10^3 m \sim 10^{16}$  GeV,  $\xi$  is needed as at least  $10^6$ . Namely, unless  $\xi$  takes a very large

value, the GUT scale boson is hard to be created. Moreover, even if  $\xi$  takes a very large value, since the Mathieu parameters  $A_k$  and  $q$  deviate from instability band due to mass effect from the very beginning, the final abundance of the  $\chi$ -particles must be very small as estimated by Eq. (3.10) as  $\langle \bar{\chi}^2 \rangle_f \propto 1/\xi$ . Finally, we show the value of  $\langle \bar{\chi}^2 \rangle_f$  as a function of  $\bar{m}_\chi$  in the case of  $\xi = 100$  in Fig. 6.  $\langle \bar{\chi}^2 \rangle_f$  is the quadratically decreasing function of  $\bar{m}_\chi$  as is expected from Eq. (3.10). We find that the  $\chi$ -particle whose mass is more than  $m_\chi \gtrsim 10m$  can not be produced, justifying the estimation (3.12).

## B. Case of $\xi < 0$

### 1. massless $\chi$ -particle case

Let us investigate the  $\xi < 0$  case for the massless  $\chi$ -particle. In the  $\xi < 0$  case,  $q$  takes negative value as is found by Eq. (3.7). Since the Mathieu chart is symmetrical with respect to  $A_k$ -axis, it is enough to consider the absolute value of  $q$ :

$$|q| = \frac{4}{3\pi\bar{t}} \left[ 3|\xi|(1 - 3\eta) + \frac{1}{2} \right]. \quad (3.13)$$

Note that  $|q|$  is larger than in the positive  $\xi$  case because of the last term  $+1/2$ , which makes the resonant more efficient. Even if  $\xi = -1$  ( $q_i \approx 1.5$ ), parametric resonance evidently occurs, although the final abundance is very small:  $\langle \bar{\chi}^2 \rangle_f = 2.63 \times 10^{-11}$  (see Fig. 7(a)). For  $\xi = -3$  ( $q_i \approx 4.0$ ), the final values are  $\bar{t}_f = 7.02$ ,  $q_f = 0.57$  and  $\langle \bar{\chi}^2 \rangle_f = 8.71 \times 10^{-5}$ . Hence parametric resonance is much more efficient than in the  $\xi = 3$  case. One characteristic property in the  $\xi < 0$  case is that  $\langle \bar{\chi}^2 \rangle$  can increase before the  $\varphi$  field enters the coherent oscillation stage. This is because the time dependent frequency  $\omega_k^2$  of Eq. (2.43) takes negative value initially for  $k = 0$ , and  $\langle \bar{\chi}^2 \rangle$  grows due to negative coupling instability. For example, in the  $\xi = -3$  case,  $\langle \bar{\chi}^2 \rangle$  decreases slightly initially by the expansion of the universe, but begins to increase after that (Fig. 7(b)). This is another factor where the negative  $\xi$  case gives more efficient preheating than the positive one. After  $\bar{t} \approx 1$ , the approximation (2.27) is valid and the analytical estimation by the Mathieu equation is relevant. The final value  $q_f$  is small for  $\xi > -3$ , we can neglect the back reaction effect and the resonance terminates by passing across the first resonant band. For  $\xi = -5$ , however, the final values are  $\bar{t}_f = 3.80$ ,  $q_f = 1.57$  and  $\langle \bar{\chi}^2 \rangle_f = 2.63 \times 10^{-4}$  (Fig. 7(c)). Since  $q_f$  is larger than unity, the backreaction by the  $\xi\eta$  term in Eq. (3.6) becomes important and one can estimate the final abundance  $\langle \bar{\chi}^2 \rangle_f$  for  $\xi \lesssim -4$  by the same method as the  $\xi > 0$  case. By using the criterion  $A_k = 3|q|$  for Eqs. (3.6) and (3.13),  $\langle \bar{\chi}^2 \rangle_f$  is estimated as



$$\langle \bar{\chi}^2 \rangle_f \approx \frac{1}{24\pi|\xi|(\pi\bar{t}_f - 1)} \left( 1 + \frac{1}{6|\xi|} \right). \quad (3.14)$$

This shows that the maximal value of  $\langle \bar{\chi}^2 \rangle_f$  becomes larger than that of the  $\xi > 0$  case in Eq. (3.7). Actually, the value of  $\langle \bar{\chi}^2 \rangle_f$  in the range  $-15 \lesssim \xi \lesssim -4$  is larger than the maximal value for  $\xi > 0$  case (See Fig. 4). For  $\xi = -10$ ,  $\langle \bar{\chi}^2 \rangle_f$  estimated by Eq. (3.14) is  $\langle \bar{\chi}^2 \rangle_f = 1.74 \times 10^{-4}$  (at  $t_f = 2.78$ ) and the numerical value is  $\langle \bar{\chi}^2 \rangle_f = 1.78 \times 10^{-4}$ . The analytic estimation (3.14) gives quite good agreement with the numerical results for  $-20 \lesssim \xi \lesssim -4$  (See Table III).

For  $\xi \lesssim -20$ , however, the final point  $\bar{t}_f$  becomes less than unity, and the estimation (3.14) based on the Mathieu equation is broken. In this case, since  $\omega_k^2$  takes negative value for most  $k$  modes,  $\langle \bar{\chi}^2 \rangle$  and  $|\eta|$  increase rapidly. Then, the term  $e^{\frac{\sqrt{6}}{3}\kappa\phi} - 1 + 3\eta$  in Eq. (2.43) decreases and becomes negative while  $\omega_k^2$  becomes positive for any  $\phi$ , which means the negative coupling instability does not occur any more. Note that the  $\phi$  field equation (2.21) includes a similar term :  $e^{\frac{\sqrt{6}}{3}\kappa\phi} - 1 + \eta$ . Although the  $\eta$  term is expected to work as the backreaction on the  $\phi$  field, the effect on the  $\chi$  field equation is dominant due to the difference by factor 3. After the inflaton field enters the coherent oscillation stage,  $A_k$  is much larger than  $|q|$  and the further resonance does not come about. By making use of this picture, we can estimate the final abundance of  $\langle \bar{\chi}^2 \rangle_f$  for  $\xi \lesssim -20$  as

$$\langle \bar{\chi}^2 \rangle_f \approx \frac{1}{24\pi|\xi|} \left( e^{\frac{\sqrt{6}}{3}\kappa\phi_f} - 1 \right), \quad (3.15)$$

where  $\phi_f = \phi(t_f)$ . For example, when  $\xi = -50$ , numerical values are  $\bar{t}_f = 0.58$ ,  $\langle \bar{\chi}^2 \rangle_f = 2.82 \times 10^{-4}$  and  $\phi_f = 0.128M_{\text{PL}}$ . Then,  $\langle \bar{\chi}^2 \rangle_f$  estimated by Eq. (3.15) is  $\langle \bar{\chi}^2 \rangle_f = 1.83 \times 10^{-4}$ . In spite of the naive estimation, it gives a value close to the numerical one. We show the final abundance  $\langle \bar{\chi}^2 \rangle_f$  for  $\xi < 0$  in Fig. 4. We can find that  $\langle \bar{\chi}^2 \rangle_f$  takes its maximum value  $\langle \bar{\chi}^2 \rangle_{\text{max}} \approx 3 \times 10^{-4}$  for  $\xi \approx -4$  (and  $\xi \approx -40$ ), which is larger than  $\xi > 0$  case. For  $\xi \lesssim -40$ ,  $\langle \bar{\chi}^2 \rangle_f$  begins to decrease by the factor:  $1/|\xi|$ .

## 2. massive $\chi$ -particle case

We investigate the  $\xi < 0$ ,  $m_\chi \neq 0$  case as the final case in this section. Since  $A_k$  and  $|q|$  are expressed as Eq. (3.6) and

$$|q| = \frac{4}{3\pi\bar{t}} \left[ 3|\xi|(1 - 3\eta) + \bar{m}_\chi^2 + \frac{1}{2} \right], \quad (3.16)$$

the mass effect makes both  $A_k$  and  $|q|$  larger than the massless case. Although the large  $q$  value gives an efficient preheating, the increase of  $A_k$  is more significant than the increase of  $|q|$ , and  $\chi$ -particle production is suppressed by

taking the mass effect into account. For example, when  $\bar{m}_\chi = 1$ , the resonance of  $\chi$ -particles can not be seen for  $-3 \lesssim \xi \lesssim 0$ . Consider the case of  $\xi = -5$  and  $\bar{m}_\chi = 1$  (See Fig. 8(a)). Although the growth rate is small,  $\langle \bar{\chi}^2 \rangle$  is slowly increasing up to  $\langle \bar{\chi}^2 \rangle_f = 3.24 \times 10^{-8}$  (at  $\bar{t}_f = 7.74$ ). In this case, since  $q_f = 0.90$  and  $36\xi\eta \ll 1$ , the resonance terminates by the expansion of the universe. When  $\xi = -10$  and  $\bar{m}_\chi = 1$ , the resonance is efficient and the final values are  $\langle \bar{\chi}^2 \rangle_f = 1.13 \times 10^{-4}$ ,  $\bar{t}_f = 2.69$  and  $q_f = 4.61$  (Fig. 8(b)). In this case, the increase of  $A_k$  due to  $\chi$ -particle production determines the final abundance. By using the same criterion as in the previous cases, we can estimate the value of  $\langle \bar{\chi}^2 \rangle_f$  as

$$\langle \bar{\chi}^2 \rangle_f \approx \frac{1}{72\pi\xi^2} \left[ \frac{6|\xi| + 1}{2(\pi\bar{t}_f - 1)} - \bar{m}_\chi^2 \right]. \quad (3.17)$$

In the  $\xi = -10$  case, the estimated value is  $\langle \bar{\chi}^2 \rangle_f = 1.37 \times 10^{-4}$ , which is close to the numerical value. Eq. (3.17) is relevant for  $-30 \lesssim \xi \lesssim -10$  because  $\bar{t}_f$  is larger than unity. However, for  $\xi \lesssim -30$ , where the resonance terminates before the inflaton field begins to oscillate coherently, we should use the estimation

$$\langle \bar{\chi}^2 \rangle_f \approx \frac{1}{24\pi|\xi|} \left( e^{\sqrt{\frac{2}{3}}\kappa\phi_f} - 1 - \frac{\bar{m}_\chi^2}{3|\xi|} \right), \quad (3.18)$$

which can be obtained similarly to Eq. (3.15). Note that Eq. (3.18) is valid when  $\bar{m}_\chi^2$  is not as large as  $|\xi|$ . If  $\bar{m}_\chi^2$  is large as compared with  $|\xi|$ ,  $\omega_k^2$  becomes positive at the initial stage by Eq. (2.43) and can not give the negative coupling instability. For example, when  $\xi = -50$  and  $\bar{m}_\chi = 1$ , the numerical values are  $\langle \bar{\chi}^2 \rangle_f = 2.79 \times 10^{-4}$ ,  $\bar{\phi}_f = 0.128 M_{\text{PL}}$  at  $\bar{t}_f = 0.58$ , while the estimated value by Eq. (3.18) is  $\langle \bar{\chi}^2 \rangle_f = 1.81 \times 10^{-4}$  (See Table IV for other examples). In this case, as is found by Eq. (3.18), the mass term does not affect a significant role. However, if  $\bar{m}_\chi$  is large,  $\langle \bar{\chi}^2 \rangle_f$  is significantly suppressed by a mass effect (Compare with  $\xi = -50$ ,  $\bar{m}_\chi = 7$  case). Since  $\chi$ -particle production is possible naively when the r.h.s. in Eq. (3.18) takes positive value, the produced mass of the  $\chi$ -particle is bounded as

$$\bar{m}_\chi \lesssim \sqrt{3|\xi| \left( e^{\sqrt{\frac{2}{3}}\kappa\phi_f} - 1 \right)}. \quad (3.19)$$

$\phi_f$  is smaller than the initial value  $M_{\text{PL}}/5$  for large  $\xi$ . This means that  $\bar{m}_\chi$  is constrained to be

$$\bar{m}_\chi \lesssim 2\sqrt{|\xi|}. \quad (3.20)$$

The massive  $\chi$ -particle whose mass is of the order  $m_\chi \sim 10^{13}$  GeV can be generated even if  $\xi \sim -5$ , but with the increase of  $m_\chi$ , the  $\chi$ -particle is hard to produce because  $m_\chi$  is strongly restricted by Eq. (3.20). In particular,  $|\xi|$  still needs to take a very large value  $|\xi| \gtrsim 10^5$  in order to produce the GUT scale gauge boson:  $m_\chi \sim 10^{16}$  GeV. As a

result, it seems difficult to produce the GUT scale particle by parametric resonance in the  $R^2$  inflation model in both the  $\xi > 0$  and  $\xi < 0$  cases.

#### IV. PREHEATING BY $R^4$ INFLATION MODEL

In this section, we consider the  $R^4$  inflation model as the next example. In the  $R^4$  inflation model, inflation is hardly realized because a fine tuning of the initial value of the inflaton field is needed and the coupling constant  $\alpha_4$  is constrained to be very large [34]. It is worth, however, investigating whether a preheating stage exists or not and how the preheating process proceeds if it occurs. In this case, the value of the inflaton when the reheating process turns on is  $\phi \approx M_{\text{PL}}/9$ . After  $\phi$  decreases under  $\phi \approx M_{\text{PL}}/20$ , the scale factor evolves as  $a \approx (t/t_0)^{5/6}$ , where  $\tau$  and  $\varphi$  are defined as  $\tau = 2t_0/3 (t/t_0)^{3/2}$  and  $\varphi = a^{9/5}\phi$ , respectively by Eqs. (2.32)-(2.34). As for the  $\varphi$  field, integrating the r.h.s. in Eq. (2.37), we find that  $\tau$  is expressed by the combination of the complete elliptic integrals of the first kind  $F(\theta, 1/\sqrt{2})$  and the second kind  $E(\theta, 1/\sqrt{2})$  [35]:

$$F\left(\theta, \frac{1}{\sqrt{2}}\right) - 2E\left(\theta, \frac{1}{\sqrt{2}}\right) = \pm \frac{2}{3} \left(\frac{K_4^3}{E}\right)^{1/4} (\tau - \tau_0), \quad (4.1)$$

where

$$\theta = \cos^{-1} \left[ \left(\frac{K_4}{E}\right)^{1/4} \varphi^{1/3} \right]. \quad (4.2)$$

Since  $F(\theta, 1/\sqrt{2})$  and  $E(\theta, 1/\sqrt{2})$  are well approximated as  $F(\theta, 1/\sqrt{2}) \approx 1.1803\theta$  and  $E(\theta, 1/\sqrt{2}) \approx 0.8598\theta$ , we obtain the evolution of the  $\varphi$  field as

$$\varphi^{1/3} \approx \varphi_0^{1/3} \cos \left[ \frac{c\sqrt{K_4}}{\varphi_0^{1/3}} (\tau - \tau_0) \right], \quad (4.3)$$

where  $c = 1.2360$  is a constant and  $\varphi_0 \equiv (E/K_4)^{3/4}$  represents the amplitude of the  $\varphi$  field. Note that the variable

$$m_4 \equiv \frac{c\sqrt{K_4}}{\varphi_0^{1/3}} \quad (4.4)$$

plays the role of the “inflaton mass” for the  $R^4$  inflation model when the inflaton field oscillates coherently.

Next, consider the evolution of the  $\chi$  field. The time dependent frequency in the present model is expressed as

$$\omega_k^2 = a^{-\frac{6}{5}} \left[ \frac{k^2}{a^2} + e^{-\frac{\sqrt{6}}{3}\kappa\phi} \left\{ \frac{8}{3} \lambda_4 \xi \kappa^2 \left( e^{\frac{\sqrt{6}}{3}\kappa\phi} - 1 + \eta \right)^{-\frac{2}{3}} \left( e^{\frac{\sqrt{6}}{3}\kappa\phi} - 1 + \frac{5}{3}\eta \right) + m_\chi^2 \right\} \right] + \frac{\kappa}{\sqrt{6}} \frac{d^2\phi}{d\tau^2} + \frac{\kappa^2}{6} \left( \frac{d\phi}{d\tau} \right)^2, \quad (4.5)$$

where we used the approximation  $\kappa \frac{d\phi}{d\tau} \gg \frac{da}{d\tau}$ . Further, adopting the approximations: Eqs. (2.27) and (2.28), the frequency can be written by

$$\omega_k^2 \approx a^{-\frac{6}{5}} \left( \frac{k^2}{a^2} + m_\chi^2 \right) + \left( \frac{2}{3} \right)^{\frac{3}{2}} a^{-\frac{9}{5}} (6\xi - 1) \kappa K_4 \varphi_0^{\frac{1}{3}} \cos[m_4(\tau - \tau_0)], \quad (4.6)$$

where we used Eq. (4.3). Setting  $2z = m_4(\tau - \tau_0) + \pi$ , Eq. (2.42) is reduced to the Mathieu equation (3.5), with

$$A_k = 4a^{-\frac{6}{5}} \left( \frac{\bar{k}^2}{a^2} + \bar{m}_\chi^2 \right), \quad (4.7)$$

$$q = c' \left( \xi - \frac{1}{6} \right) a^{-\frac{9}{5}} \bar{\varphi}_0, \quad (4.8)$$

where  $c' \equiv \frac{32}{c^2} \sqrt{\frac{\pi}{3}} = 21.4338$ ,  $\bar{k} \equiv k/m_4$ ,  $\bar{m}_\chi \equiv m_\chi/m_4$  and  $\bar{\varphi}_0 \equiv \varphi_0/M_{\text{PL}}$ . Both of the Mathieu parameters decrease by the expansion of the universe in the  $R^4$  model. Note that this relation can only be used for  $\eta \ll 1$ . As  $\chi$ -particles are produced, we have to take into account the suppression effect by the increase of  $|\eta|$ . As the  $R^2$  inflation model, the difference between the  $\xi > 0$  and  $\xi < 0$  cases appears in the sign of the term  $1/6$  in Eq. (4.8). This difference, however, is not important for  $|\xi| \gg 1$ .

The expectation value  $\langle \chi^2 \rangle$  is normalized as

$$\langle \bar{\chi}^2 \rangle \equiv \frac{\langle \chi^2 \rangle}{M_{\text{PL}}^2} = \left( \frac{m_4}{M_{\text{PL}}} \right)^2 \frac{1}{2\pi^2} \int \bar{k}^2 |\bar{\chi}_k|^2 d\bar{k} = \frac{c^2}{16(12\pi\bar{\varphi}_0)^{\frac{2}{3}}\beta^{\frac{1}{3}}} \frac{1}{2\pi^2} \int \bar{k}^2 |\bar{\chi}_k|^2 d\bar{k}, \quad (4.9)$$

where  $\bar{\chi}_k \equiv \sqrt{m_4} \chi_k$ . Since  $\beta$  is strongly constrained as Eq. (2.18), the normalized value of  $\langle \bar{\chi}^2 \rangle$  is very small initially. However, since  $\langle \bar{\chi}^2 \rangle$  can grow exponentially by the parametric resonance, we can expect a considerable amount of the  $\chi$ -particles at the final stage of the preheating. We use a dimensionless time parameter defined by  $\tilde{t} \equiv M_{\text{PL}} \beta^{-\frac{1}{6}} t$  in numerical calculations. Counting time from  $\phi \approx M_{\text{PL}}/9$ , the evolution of the  $\varphi$  field is described by Eq. (4.3) with  $\varphi_0 \approx 0.05 M_{\text{PL}}$  (at  $\tilde{t}_0 \approx 20$ ). Then Eq. (4.8) is rewritten as

$$q \approx 1.0716 \left( \xi - \frac{1}{6} \right) \left( \frac{\tilde{t}}{20} \right)^{-\frac{3}{2}}. \quad (4.10)$$

We find from this relation that  $q$  decreases faster as compared with the  $R^2$  inflation model.

First, consider the  $\xi > 0$  case for the massless  $\chi$ -particles. For  $0 \lesssim \xi \lesssim 3$ ,  $\langle \bar{\chi}^2 \rangle$  does not increase because the initial value of  $q$  is small. For  $\xi \gtrsim 5$ , however, we can see that  $\langle \bar{\chi}^2 \rangle$  grows by the parametric resonance. Consider the case of  $\xi = 10$  (See Fig. 9(a)). Numerically, the final values are  $\tilde{t}_f = 161$  and  $\langle \bar{\chi}^2 \rangle_f = 5.89 \times 10^{-27}$  (See Table IV). Although the total amount of created  $\chi$ -particles is not large because of the small initial value, parametric resonance evidently occurs due to the oscillating  $\varphi$  field. In this case, since  $\eta$  is much smaller than unity, the backreaction effect due to  $\chi$ -particle production does not affect the  $\chi$ -field evolution. When the Mathieu parameters with low momentum, which

contribute the resonance mainly, pass across the first instability band by Hubble expansion, the resonance terminates. In the case of  $\xi = 30$ , the final values are  $\tilde{t}_f = 185$  and  $\langle \bar{\chi}^2 \rangle = 1.29 \times 10^{-5}$  (Fig. 9(b)). In spite of the small initial fluctuation,  $\langle \bar{\chi}^2 \rangle$  increases up to  $\langle \bar{\chi}^2 \rangle_f \sim 10^{-5}$  by copious production of the  $\chi$ -particles. In the case of  $\xi = 50$ , the final values are  $\tilde{t}_f = 140$  and  $\langle \bar{\chi}^2 \rangle_f = 8.28 \times 10^{-6}$  (Fig. 9(c)). Although the growth rate of  $\langle \bar{\chi}^2 \rangle$  becomes larger than the  $\xi = 30$  case because of the large initial value of  $q$ , the final abundance is almost the same. This means that the suppression effect by the backreaction is significant when the fluctuation increases up to  $\langle \bar{\chi}^2 \rangle \sim 10^{-5}$ . In such cases, we can estimate the final abundance of  $\chi$ -particles as follows. When  $\eta \ll 1$ , the time dependent frequency (4.5) can become negative for  $\phi \lesssim 0$  and the  $\chi$ -particle can be produced by the negative coupling instability. However as the  $\chi$ -particles are produced enough, the second term in the square bracket of Eq. (4.5) becomes positive for any value of  $\phi$ . We can roughly estimate that the resonance finally terminates when  $\eta$  grows up to

$$\frac{5}{3}\eta \approx e^{\frac{\sqrt{6}}{3}\kappa\Phi} - 1 \approx \frac{\sqrt{6}}{3}\kappa\Phi \approx \frac{\sqrt{6}}{3}\kappa \left(\frac{t_f}{t_0}\right)^{-\frac{3}{2}} \varphi_0, \quad (4.11)$$

where we used the relation  $\Phi_f \approx \left(\frac{t_f}{t_0}\right)^{-\frac{3}{2}} \varphi_0$ .  $\Phi$  represents the amplitude of  $\phi$ . Namely,

$$\langle \bar{\chi}^2 \rangle_f \approx \frac{1}{10\xi} \sqrt{\frac{3}{\pi}} \left(\frac{\tilde{t}_f}{t_0}\right)^{-\frac{3}{2}} \bar{\varphi}_0. \quad (4.12)$$

Let us adopt the values of  $\bar{\varphi}_0 = 0.05$  and  $\tilde{t}_0 = 20$ . For the  $\xi = 30$  and  $\xi = 50$  cases,  $\langle \bar{\chi}^2 \rangle_f$  estimated by Eq. (4.12) are  $\langle \bar{\chi}^2 \rangle_f = 5.79 \times 10^{-6}$  and  $\langle \bar{\chi}^2 \rangle_f = 5.28 \times 10^{-6}$ , respectively (Other examples are listed in Table V). In spite of the naive estimation of Eq. (4.12), it gives fairly close values to the numerical ones. We did not take into account the  $d^2\phi/d\tau^2$  term in Eq (4.5) for the estimation. This is one of the reasons why the analytical values are smaller than the numerical values. Note that the r.h.s in Eq. (4.12) can be regarded as the function of two variables  $\xi$  and  $t_f$ . With the increase of  $\xi$ , numerical calculation shows that  $t_f$  decreases. For  $25 \lesssim \xi \lesssim 100$ , the decreasing rate  $1/\xi$  of  $\langle \bar{\chi}^2 \rangle_f$  almost balances with the increasing rate  $(t_f/t_0)^{-\frac{3}{2}}$ . Hence  $\langle \bar{\chi}^2 \rangle_f$  takes almost constant value  $\langle \bar{\chi}^2 \rangle_f \approx (1 \sim 3) \times 10^{-5}$  (See Fig. 10). To be more precise,  $\langle \bar{\chi}^2 \rangle_f$  takes the maximal value  $\langle \bar{\chi}^2 \rangle_f \approx 3 \times 10^{-5}$  for  $\xi \approx 40$ . For  $\xi \gtrsim 100$ , the decreasing rate  $1/\xi$  surpasses the increasing rate  $\left(\frac{t_f}{t_0}\right)^{-\frac{3}{2}}$  and  $\langle \bar{\chi}^2 \rangle_f$  decreases with the increase of  $\xi$ .

Next, we consider the  $\xi < 0$  case for the massless  $\chi$ -particles. In this case, since the absolute value of  $q$  is represented as

$$|q| = c' \left( |\xi| + \frac{1}{6} \right) \left( \frac{t}{t_0} \right)^{-\frac{3}{2}} \bar{\varphi}_0, \quad (4.13)$$

the initial value of  $|q|$  is slightly larger than the  $\xi > 0$  case. Moreover, since  $\omega_k^2$  in Eq. (4.5) can take negative value from

the first stage of preheating,  $\langle \bar{\chi}^2 \rangle$  grows rather effectively. Numerically, while  $\langle \bar{\chi}^2 \rangle$  does not increase for  $-3 \lesssim \xi \lesssim 0$  at all, the growth of  $\langle \bar{\chi}^2 \rangle$  is expected for  $\xi \lesssim -3$ . For example, in the case of  $\xi = -5$ ,  $\langle \bar{\chi}^2 \rangle$  increases exponentially and reaches the final value  $\langle \bar{\chi}^2 \rangle_f = 1.95 \times 10^{-33}$  at  $\tilde{t}_f = 100$  (Fig. 11(a)). At the initial stage,  $\langle \bar{\chi}^2 \rangle$  decreases slightly by the Hubble expansion, and then increases due to negative instability from  $\tilde{t} \approx 10$ , which is earlier than the  $\xi > 0$  case. The smaller the value of  $\xi$  we adopt, the larger the final abundance  $\langle \bar{\chi}^2 \rangle_f$  becomes, and it reaches a plateau when  $\xi \approx -20$ . In the case of  $\xi = -20$ , the final values are  $\tilde{t}_f = 156$  and  $\langle \bar{\chi}^2 \rangle_f = 3.08 \times 10^{-5}$  (Fig. 11(b)). As  $\xi$  further decreases under  $\xi \approx -20$ , the suppression effect by  $\chi$ -particle production begins to work, and  $\langle \bar{\chi}^2 \rangle_f$  does not increase while the growth rate becomes large as the decrease of  $\xi$ . Numerically,  $\langle \bar{\chi}^2 \rangle_f$  takes almost constant value  $\langle \bar{\chi}^2 \rangle_f \approx (2 \sim 5) \times 10^{-5}$  for the range  $-100 \lesssim \xi \lesssim -20$ . For example, in the case of  $\xi = -50$ , the final values are  $\tilde{t}_f = 82$  and  $\langle \bar{\chi}^2 \rangle_f = 2.18 \times 10^{-5}$  (Fig. 11(c)). We can estimate  $\langle \bar{\chi}^2 \rangle_f$  in the same way as the  $\xi > 0$  case, which yields

$$\langle \bar{\chi}^2 \rangle_f \approx \frac{1}{10|\xi|} \sqrt{\frac{3}{\pi}} \left( \frac{t_f}{t_0} \right)^{-\frac{3}{2}} \bar{\varphi}_0. \quad (4.14)$$

When  $\xi = -50$ ,  $\langle \bar{\chi}^2 \rangle_f$  estimated by Eq. (4.14) is  $\langle \bar{\chi}^2 \rangle_f = 1.18 \times 10^{-5}$ , which is close to the numerical value  $\langle \bar{\chi}^2 \rangle_f = 2.18 \times 10^{-5}$ . In the case of  $\xi \lesssim -100$ , the factor  $1/|\xi|$  becomes dominant and  $\langle \bar{\chi}^2 \rangle_f$  decreases with the increase of  $|\xi|$ . In Table VI, we show the numerical and analytical values by Eq. (4.14) in various cases. We also depict the numerical value of  $\langle \bar{\chi}^2 \rangle_f$  as a function of  $\xi$  in Fig. 10. We find that  $\langle \bar{\chi}^2 \rangle_f$  takes almost constant value for  $-100 \lesssim \xi \lesssim -20$ . The achieved maximal fluctuation in the  $R^4$  inflation model is  $\langle \bar{\chi}^2 \rangle_{max} \approx 5 \times 10^{-5}$  at  $\xi \approx -35$ , which is smaller than that in the  $R^2$  inflation model.

Finally, we take the mass of the  $\chi$ -particles into account. In the  $R^2$  inflation model,  $A_k$  is constrained as  $A_k \geq 4\bar{m}_\chi^2$  throughout the preheating. In the  $R^4$  inflation model, although  $A_k$  increases by the mass term similarly, it can decrease due to the prefactor  $a^{-6/5}$  and the system might give a resonance which is not inefficient compared with the massless case. However, we have to note that  $q$  value decreases by the Hubble expansion simultaneously. If  $q$  decreases faster than  $A_k$ , the parametric resonance is suppressed as in the  $R^2$  inflation model. Unfortunately, this is the case. As one example, we show the  $\langle \bar{\chi}^2 \rangle$  evolution in the case of  $\xi = -50$ ,  $m_\chi = m_4$  in Fig. 12. We find that the growth of  $\langle \bar{\chi}^2 \rangle$  is strongly suppressed by the mass effect. Although  $A_k$  and  $q$  in Eq. (4.7) and (4.8) are not written by the forms which include the term  $\eta$ , we can roughly estimate the maximal value of  $m_\chi$  by using the criterion:  $A_k \lesssim 3q$ . Considering the  $k = 0$  mode,  $\bar{m}_\chi$  is constrained as

$$\bar{m}_\chi \lesssim \sqrt{\frac{\xi}{2}} \left( \frac{\bar{t}}{20} \right)^{-\frac{1}{4}}. \quad (4.15)$$

The above estimation gives a much lower upper bound than that in the  $R^2$  inflation case. From Eq. (4.15), the  $\chi$ -particle whose mass is of the order  $m_\chi \sim m_4 \sim 3 \times 10^{-22} M_{\text{PL}}$  can be produced if  $|\xi| \gtrsim 100$ . We conclude that an unnaturally large value of  $|\xi|$  is needed even if GeV scale bosons are to be produced.

## V. CONCLUSIONS AND DISCUSSIONS

In this paper, we analyze preheating with non-minimally coupled scalar field  $\chi$  in the higher-curvature inflation model. We have examined properties of resonance, especially for  $R^2$ - and  $R^4$ -inflation models. In the  $R^2$  model,  $R^2$ -term provides us an effective inflaton field  $\phi$ , and inflation is realized through the flat plateau for  $\phi \gtrsim M_{\text{PL}}$ . In the reheating phase, the  $\phi$  field behaves as a massive scalar field. Although the evolutions of scale factor and  $\phi$  field in the present model are almost the same as those for a massive inflaton with  $V(\phi) = \frac{1}{2}m^2\phi^2$  in the non-minimal coupling  $\frac{1}{2}\xi R\chi^2$  case, the structure of resonance is different. In the  $R^2$  model, since the resonance parameter  $q$  decreases as  $1/t$  due to the expansion of the universe, which is slower than that in the model with  $V(\phi, \chi) = \frac{1}{2}m^2\phi^2 + \frac{1}{2}\xi R\chi^2$ , we do not need so large a value of  $|\xi|$  as  $|\xi| \gtrsim 10$  for an effective resonance. In the  $\xi > 0$  case with a massless  $\chi$ -particle, if  $\xi$  is larger than  $\xi \gtrsim 1$ ,  $\chi$ -particle production is possible against the diluting effect by cosmic expansion. When  $1 \lesssim \xi \lesssim 5$ , the total amount of created  $\chi$ -particles  $\langle \chi^2 \rangle_f$  grows with the increase of  $\xi$ , because the initial value of  $q$  becomes larger. However, for  $\xi \gtrsim 5$ ,  $\langle \chi^2 \rangle_f$  slowly decreases as the increase of  $\xi$  because of the suppression effect by  $\chi$ -particle production. Hence, in the positive  $\xi$  case,  $\langle \chi^2 \rangle_f$  takes the maximal value  $\sqrt{\langle \chi^2 \rangle_{\text{max}}} \approx 1.5 \times 10^{17}$  GeV at  $\xi \approx 5$ . When  $\xi$  is negative, the resonance structure does not change so much except for the small increase of the  $|q|$  value. In this case, the  $\chi$ -particle production becomes possible for  $\xi \lesssim -1$ . For  $-4 \lesssim \xi \lesssim -1$ ,  $\langle \chi^2 \rangle_f$  increases with the decrease of  $\xi$ , and  $\langle \chi^2 \rangle_f$  takes maximal value  $\sqrt{\langle \chi^2 \rangle_{\text{max}}} \approx 2 \times 10^{17}$  GeV at  $\xi \approx -4$ . For the case of  $\xi \lesssim -20$ , a  $\chi$ -particle fluctuation rapidly grows with the passage of time and reaches the maximal value  $\langle \chi^2 \rangle_f$  before the  $\phi$ -field begins to oscillate sinusoidally. This means that in the  $\xi < 0$  case, the effective  $\chi$ -particle production occurs due to a negative coupling instability irrespective of the coherent oscillation of  $\phi$ -field. Numerically,  $\langle \chi^2 \rangle_f$  slowly increases for  $-40 \lesssim \xi \lesssim -20$  with the decrease of  $\xi$ , and the value of  $\langle \chi^2 \rangle_f$  in the  $\xi \approx -40$  case is almost the same as the  $\xi \approx -4$  case. In summary, in the  $R^2$  model, the achieved maximal value of  $\chi$ -particle fluctuation is  $\sqrt{\langle \chi^2 \rangle_{\text{max}}} \approx 2 \times 10^{17}$  GeV for  $\xi \approx -4$  (and  $\xi \approx -40$ ). As for the massive  $\chi$ -particle case, a parametric resonance is suppressed by the mass effect. We find the relation for the massive  $\chi$ -particle production to occur:  $\bar{m}_\chi \lesssim \sqrt{\xi}$  for  $\xi > 0$  and  $\bar{m}_\chi \lesssim 2\sqrt{|\xi|}$  for  $\xi < 0$ . Hence it is difficult to produce GUT scale gauge bosons unless  $|\xi|$  is as enormously large as  $|\xi| \gtrsim 10^5$ .

As for the  $R^4$  model, inflation is difficult to realize unless selecting the very large coupling constant  $\alpha_4$  with spacetime curvature. Nevertheless, we have examined the resonance structure, because we are interested in whether a preheating stage generally exists or not for  $n > 2$ . Since the potential of the  $\phi$  field is written as  $V(\phi) \sim \phi^{\frac{4}{3}}$  for  $\phi \lesssim M_{\text{PL}}/20$ , the oscillation of the  $\phi$  field is not exactly sinusoidal. However, we find that the behavior of  $\phi$  field is well approximated as a sinusoidal oscillation, and the equation of the  $\chi$  field is reduced to the Mathieu equation. In the  $R^4$  case, the resonance structure changes and  $q$  decreases as  $q \sim t^{-\frac{3}{2}}$ , which is faster than the  $R^2$  case. For  $\xi \gtrsim 5$  and  $\xi \lesssim -3$ , the fluctuation of  $\chi$ -particles grows with the passage of time. However,  $\langle \bar{\chi}^2 \rangle_f$  is rather small for  $|\xi| \lesssim 20$ , because a parametric resonance is not so effective. For  $20 \lesssim |\xi| \lesssim 100$ ,  $\langle \chi^2 \rangle_f$  takes the almost constant value  $\sqrt{\langle \chi^2 \rangle_f} \approx (4 \sim 8) \times 10^{16}$  GeV, and for  $|\xi| > 100$ ,  $\langle \chi^2 \rangle_f$  decreases with the increase of  $|\xi|$ . The maximum value achieved in the  $R^4$  model is  $\sqrt{\langle \chi^2 \rangle_f} \approx 8 \times 10^{16}$  GeV at  $\xi \approx -35$ . Taking into account the mass effect of  $\chi$ -particles, the final fluctuation is more strongly suppressed as compared with the  $R^2$  inflation model.

As for  $R^n (n > 4)$  model, the coupling constant  $\alpha_n$  is constrained to be very large as Eq. (2.16). Although this model is rather unnatural, we should stress that it is still possible to investigate the resonance structure by the same method as in the  $n = 4$  case. The oscillation of the  $\phi$  field around the potential Eq. (2.8) is approximately written by the sinusoidal form, so the fluctuation of  $\chi$ -particles can grow by a parametric resonance. Hence, in this sense, a preheating stage generically exists in the higher-curvature inflation model with a non-minimal coupling, irrespective of the problem of the large coupling constant.

In a higher-curvature inflation model, inflation is realized through the coupling with spacetime curvature. Because of this, the inflaton field is the product of a purely gravitational source. Hence for the complete study of preheating, we should take into account the metric perturbation. It was pointed out in Ref. [36–41] that the metric perturbation undergoes the effect of parametric resonance in a reheating phase. Although it is rather difficult to study preheating in the present model by taking into account metric perturbations, it is of interest how the preheating dynamics are modified by this effect.

In our study of amplification of a scalar field  $\chi$  coupled non-minimally to a spacetime curvature  $R$  ( $\frac{1}{2}\xi R\chi^2$ ) in a higher-curvature inflation model ( $R + \alpha_n R^n$ ), we have found that the value of  $\xi$  does not need to be so large as in the case of massive inflaton plus non-minimally coupled scalar field  $\chi$  to have an effective resonance. In other gravitational theories such as the Brans-Dicke theory [42] and the induced gravity [43], we may have different types of preheating dynamics. Recently, Mazumdar and Mendes [44] studied preheating in the Brans-Dicke theory with a



model of massive inflaton plus a minimally coupled scalar field  $\sigma$  and found that the Brans-Dicke field as well as the  $\sigma$  field undergoes the effect of parametric resonance. It is of interest to investigate the amplification of a non-minimally coupled scalar field in Generalized Einstein Theories. Furthermore, although we mainly concentrate on the  $\chi$ -particle production in this paper, we may discuss an inflaton particle production with a model of some inflaton potential and non-minimally coupled scalar field  $\phi$  as well. These issues are under consideration.

#### **ACKNOWLEDGEMENTS**

T. T. is thankful for financial support from the JSPS. This work was partially supported by a Grant-in-Aid for Scientific Research Fund of the Ministry of Education, Science and Culture (No. 09410217 and Specially Promoted Research No. 08102010), by a JSPS Grant-in-Aid (No. 094162), and by the Waseda University Grant for Special Research Projects.

- 
- [1] A. H. Guth, Phys. Rev. D **23**, 347 (1981); K. Sato, Mon. Not. R. Astron. Soc. **195**, 467 (1981); Phys. Lett. **99B**, 66 (1981).
  - [2] E. W. Kolb and M. S. Turner, *The Early Universe* (Addison-Wesley, Redwood City, California, 1990); A. D. Linde, *Particle Physics and Inflationary Cosmology* (Harwood, Chur, Switzerland, 1990).
  - [3] A. Albrecht and P. J. Steinhardt, Phys. Rev. Lett. **48**, 1220 (1982).
  - [4] A. D. Linde, Phys. Lett. **108B**, 389 (1982).
  - [5] A. D. Linde, Phys. Lett. **129B**, 177 (1983).
  - [6] A. A. Starobinsky, Phys. Lett. **91B**, 99 (1980); Pis'ma Astron. Zh. **10**, 323 (1984).
  - [7] M. B. Mijić, M. S. Morris, and W. M. Suen, Phys. Rev. D **34**, 10 (1986); **34**, 2934 (1986); S. W. Hawking and J. C. Luttrell, Nucl. Phys. **B247**, 280 (1984); L. A. Kofman, V. F. Mukhanov, and D. Yu. Pogosyan, Sov. Phys. JETP **66**, 433; K. Maeda, Phys. Rev. D **37**, 858 (1988).
  - [8] A. D. Dolgov and A. D. Linde, Phys. Lett. **116B**, 329 (1982); L. F. Abbott, E. Fahri, and M. Wise, Phys. Lett. **117B**, 29 (1982).
  - [9] J. Traschen and R. H. Brandenberger, Phys. Rev. D **42**, 2491 (1990); Y. Shatanov, J. Traschen, and R. H. Brandenberger, Phys. Rev. D **51**, 5438 (1995).
  - [10] L. Kofman, A. Linde, and A. A. Starobinsky, Phys. Rev. Lett. **73**, 3195 (1994).
  - [11] D. Boyanovsky, H. J. de Vega, R. Holman, D. S. Lee, and A. Singh, Phys. Rev. D **51**, 4419 (1995); D. Boyanovsky, M. D'Attanasio, H. J. de Vega, R. Holman, D. S. Lee, and A. Singh, Phys. Rev. D **52**, 6805 (1995); D. Boyanovsky, H. J. de Vega, R. Holman, D. S. Lee, and A. Singh, J. F. J. Salgado, Phys. Rev. D **54**, 7570 (1996); D. Boyanovsky, D. Cormier, H. J. de Vega, R. Holman, A. Singh, and M. Srednicki, Phys. Rev. D **56**, 1939 (1997); D. Boyanovsky, R. Holman, S. Prem Kumar, Phys. Rev. D **56**, 1958 (1997).
  - [12] D. I. Kaiser, Phys. Rev. D **53**, 1776 (1995); D. I. Kaiser, Phys. Rev. D **56**, 706 (1997).
  - [13] D. T. Son, Phys. Rev. D **54**, 3745 (1996).
  - [14] M. Yoshimura, Prog. Theor. Phys. **94**, 873 (1995); H. Fujisaki, K. Kumekawa, M. Yamaguchi, and M. Yoshimura, Phys. Rev. D **53**, 6805 (1996); H. Fujisaki, K. Kumekawa, M. Yamaguchi, and M. Yoshimura, Phys. Rev. D **54**, 2494 (1996).
  - [15] J. Schwinger, J. Math. Phys. **2**, 407 (1961); P. M. Bakshi and K. T. Mahanthappa, J. Math. Phys. **4**, 1 (1963); L. V. Keldysh, Sov. Phys. JETP **20**, 1018 (1965).
  - [16] R. D. Jordan, Phys. Rev. D **33**, 444 (1986).
  - [17] E. Calzetta and B. L. Hu, Phys. Rev. D **35**, 495 (1987); E. Calzetta and B. L. Hu, Phys. Rev. D **37**, 2878 (1988).
  - [18] S. Khlebnikov and I. I. Tkachev, Phys. Rev. Lett. **77**, 219 (1996).
  - [19] S. Khlebnikov and I. I. Tkachev, Phys. Lett. **B390**, 80 (1997).
  - [20] S. Khlebnikov and I. I. Tkachev, Phys. Rev. Lett. **79**, 1607 (1997).
  - [21] T. Prokopec and T. G. Roos, Phys. Rev. D **55**, 3768 (1997).
  - [22] L. Kofman, A. Linde, and A. A. Starobinsky, Phys. Rev. D **73**, 3258 (1997).
  - [23] P. B. Green, L. Kofman, A. Linde, and A. A. Starobinsky, Phys. Rev. D **56**, 6175 (1997).
  - [24] W-M. Suen and P. R. Anderson, Phys. Rev. D **35**, 2940 (1987).
  - [25] B. A. Bassett and S. Liberati, Phys. Rev. D **58** 021302 (1998).
  - [26] S. Tsujikawa, K. Maeda, and T. Torii, hep-ph/9901306, to appear in Phys. Rev. D.
  - [27] E. W. Kolb, A. D. Linde, and A. Riotto, Phys. Rev. Lett. **77**, 3716 (1996); E. W. Kolb, A. Riotto, and I. I. Tkachev, Phys. Lett. **B423**, 348 (1998).
  - [28] L. Kofman, A. Linde, and A. A. Starobinsky, Phys. Rev. Lett. **76**, 1011 (1996); I. I. Tkachev, Phys. Lett. **B376**, 35 (1996); S. Kasuya and M. Kawasaki, Phys. Rev. D **56**, 7597 (1997).
  - [29] S. Khlebnikov, L. Kofman, A. Linde, and I. I. Tkachev, Phys. Rev. Lett. **81**, 2012 (1998); I. I. Tkachev, S. Khlebnikov, L. Kofman, A. Linde, Phys. Lett. **B440**, 262 (1998); S. Kasuya and M. Kawasaki, Phys. Rev. D **58**, 083516 (1998).
  - [30] G. Magnano, M. Ferraris and M. Francaviglia, Gen. Rel. Grav. **19**, 465 (1987); M. Ferraris, M. Francaviglia and G. Magnano, Class. Quantum Grav. **7**, 261 (1990); A. Jakubiec and J. Kijowski, Phys. Rev. D **37**, 1406 (1988); K. Maeda, J. A. Stein-Schabes, and T. Futamase, Phys. Rev. D **39**, 2848 (1989); K. Maeda, Phys. Rev. D **39**, 3159 (1989).
  - [31] D. H. Lyth, Phys. Rev. D **31**, 1792 (1985); A. R. Liddle and D. H. Lyth, Phys. Rep. **231**, 1 (1993).
  - [32] Our treatment in this paper is based on investigating the scalar field dynamics in the Einstein frame by making use of the mean field approximation. In order to obtain the precise results, we should perform the fully non-linear calculation in the original frame.
  - [33] N. W. Mac Lachlan, *Theory and Applications of Mathieu Functions* (Dover, New York, 1961).
  - [34] J. Ellis, N. Kaloper, K. A. Olive, and J. Yokoyama, Phys. Rev. D **59** 103503 (1999).
  - [35] A. Erdelyi *et al.*, *Higher Transcendental Functions* (McGraw-Hill, New York, 1955).
  - [36] H. Kodama and T. Hamazaki, Prog. Theor. Phys. **96**, 949 (1996); T. Hamazaki and H. Kodama, Prog. Theor. Phys. **96**, 1123 (1996).

- [37] Y. Nambu and A. Taruya, Prog. Theor. Phys. **97**, 83 (1997).
- [38] B. A. Bassett, D. I. Kaiser, and R. Maartens, hep-ph/9808404, to appear in Phys. Lett. **B**.
- [39] B. A. Bassett, F. Tamburini, D. I. Kaiser, and R. Maartens, hep-ph/9901319.
- [40] F. Finelli and R. Brandenberger, Phys. Rev. Lett. **82**, 1362 (1999).
- [41] M. Parry and R. Easther, Phys. Rev. D **59** 061301 (1999).
- [42] C. Brans and R. H. Dicke, Phys. Rev. **124**, 925 (1961); D. La and P. J. Steinhardt, Phys. Rev. Lett. **62**, 376 (1989); A. Berkin, K. Maeda, J. Yokoyama, Phys. Rev. Lett. **65**, 141 (1990); J. D. Barrow and K. Maeda, Nucl. Phys. **B341**, 294 (1990); A. Berkin and K. Maeda, Phys. Rev. D **44**, 1691 (1991); A. D. Linde, Phys. Lett. **B238**, 160 (1990); A. D. Linde, Phys. Rev. D **49**, 748 (1994); J. Garcia-Bellido, A. D. Linde, and D. A. Linde, Phys. Rev. D **50**, 730 (1994).
- [43] A. Zee, Phys. Rev. Lett. **42**, 417 (1979); S. L. Adler, Phys. Lett. **95B**, 241 (1980); S. L. Adler, Rev. Mod. Phys. **54**, 729 (1982); F. S. Accetta, D. J. Zoller, and M. S. Turner, Phys. Rev. D **31**, 3046 (1985); J. L. Cervantes-Cota and H. Dehnen, Nucl. Phys. **B442**, 391 (1995); J. L. Cervantes-Cota and H. Dehnen, Phys. Rev. D **51**, 395 (1995).
- [44] A. Mazumdar and L. E. Mendes, hep-ph/9902274.

TABLE I. The final values  $\langle\bar{\chi}^2\rangle_f$  obtained by the analytical estimation and by the numerical calculation for  $\xi > 0, m_\chi = 0$  in the case of the  $R^2$  inflation model. The analytical estimation gives a good approximation to the numerical results.  $\langle\bar{\chi}^2\rangle_{numerical}$  takes the maximal value at  $\xi \sim 5$ . We also show the time  $\bar{t}_f$  when the resonance stops and the value of  $36\xi\eta$  which indicates a suppression effect. For large values of  $\xi$ , the suppression effect by  $\chi$ -particle production is significant.

$\xi$	$\bar{t}_f$	$\langle\bar{\chi}^2\rangle_{analytic}$	$\langle\bar{\chi}^2\rangle_{numerical}$	$36\xi\eta_{numerical}$
3	5.61	—	$2.21 \times 10^{-8}$	$1.80 \times 10^{-4}$
5	6.27	$1.24 \times 10^{-4}$	$1.74 \times 10^{-4}$	3.94
10	4.28	$9.02 \times 10^{-5}$	$9.95 \times 10^{-5}$	9.00
30	2.15	$5.67 \times 10^{-5}$	$7.50 \times 10^{-5}$	$6.10 \times 10^1$
50	1.30	$5.20 \times 10^{-5}$	$2.90 \times 10^{-5}$	$6.56 \times 10^1$
100	1.15	$2.87 \times 10^{-5}$	$2.51 \times 10^{-5}$	$2.27 \times 10^2$
500	1.06	$6.13 \times 10^{-6}$	$7.96 \times 10^{-6}$	$1.80 \times 10^3$

TABLE II. The final values  $\langle\bar{\chi}^2\rangle_f$  obtained by the analytical estimation and by the numerical calculation for  $\xi > 0, m_\chi \neq 0$  in the case of the  $R^2$  inflation model. The mass effect suppresses the final  $\chi$ -particle abundance, and massive  $\chi$ -particle which does not satisfy the condition Eq. (3.14) can not be created.

$\xi$	$\bar{m}_\chi$	$\langle\bar{\chi}^2\rangle_{analytic}$	$\langle\bar{\chi}^2\rangle_{numerical}$	$\bar{t}_f$
5	1	—	$3.80 \times 10^{-12}$	6.27
10	1	—	$1.17 \times 10^{-5}$	9.22
20	1	$4.80 \times 10^{-5}$	$5.19 \times 10^{-5}$	3.23
50	2	$2.80 \times 10^{-5}$	$2.51 \times 10^{-5}$	2.08
100	3	$2.36 \times 10^{-5}$	$2.32 \times 10^{-5}$	1.21
500	10	$3.87 \times 10^{-6}$	$3.80 \times 10^{-6}$	1.18

TABLE III. The final values  $\langle\bar{\chi}^2\rangle_f$  obtained by the analytical estimation and by the numerical calculation for  $\xi < 0, m_\chi = 0$  in the case of the  $R^2$  inflation model. The analytical estimation gives a good approximation to the numerical results. We also show the time  $\bar{t}_f$  when the resonance stops and the value of  $36\xi\eta$  which indicates a suppression effect.  $\langle\bar{\chi}^2\rangle_{numerical}$  takes the maximal value at  $\xi \approx -4$  and  $\xi \approx -40$ .

$\xi$	$\bar{t}_f$	$\langle\bar{\chi}^2\rangle_{analytic}$	$\langle\bar{\chi}^2\rangle_{numerical}$	$36\xi\eta_{numerical}$
-3	7.02	—	$8.71 \times 10^{-5}$	0.71
-5	3.80	$2.51 \times 10^{-4}$	$2.63 \times 10^{-4}$	5.95
-10	2.78	$1.74 \times 10^{-4}$	$1.78 \times 10^{-4}$	$1.61 \times 10^1$
-30	0.70	$1.71 \times 10^{-4}$	$2.79 \times 10^{-4}$	$2.27 \times 10^2$
-50	0.58	$1.83 \times 10^{-4}$	$2.82 \times 10^{-4}$	$6.38 \times 10^2$
-100	0.58	$9.13 \times 10^{-5}$	$1.22 \times 10^{-4}$	$1.10 \times 10^3$
-500	0.37	$3.19 \times 10^{-5}$	$5.31 \times 10^{-5}$	$1.20 \times 10^4$

TABLE IV. The final values  $\langle \bar{\chi}^2 \rangle_f$  obtained by the analytical estimation and by the numerical calculation for  $\xi < 0, m_\chi \neq 0$  in the case of the  $R^2$  inflation model. The mass effect suppresses the final  $\chi$ -particle abundance, and massive  $\chi$ -particle which does not satisfy the condition Eq. (3.22) can not be created.

$\xi$	$m_\chi$	$\langle \bar{\chi}^2 \rangle_{analytic}$	$\langle \bar{\chi}^2 \rangle_{numerical}$	$\bar{t}_f$
-5	1	—	$3.24 \times 10^{-8}$	7.74
-10	1	$1.37 \times 10^{-4}$	$1.13 \times 10^{-4}$	2.69
-30	3	$9.46 \times 10^{-5}$	$1.58 \times 10^{-4}$	0.73
-50	7	$3.45 \times 10^{-5}$	$5.01 \times 10^{-5}$	0.67
-100	10	$6.75 \times 10^{-5}$	$8.67 \times 10^{-5}$	0.52
-500	30	$1.59 \times 10^{-5}$	$8.91 \times 10^{-6}$	0.37

TABLE V. The final values  $\langle \bar{\chi}^2 \rangle_f$  obtained by the analytical estimation and by the numerical calculation for  $\xi > 0, m_\chi = 0$  in the case of the  $R^4$  inflation model.

$\xi$	$\bar{t}_f$	$\langle \bar{\chi}^2 \rangle_{analytic}$	$\langle \bar{\chi}^2 \rangle_{numerical}$
10	161	—	$5.89 \times 10^{-27}$
30	185	$5.79 \times 10^{-6}$	$1.29 \times 10^{-5}$
50	140	$5.28 \times 10^{-6}$	$8.28 \times 10^{-6}$
70	112	$5.27 \times 10^{-6}$	$1.09 \times 10^{-5}$
100	88	$5.29 \times 10^{-6}$	$1.06 \times 10^{-5}$
300	59	$3.21 \times 10^{-6}$	$5.37 \times 10^{-6}$

TABLE VI. The final values  $\langle \bar{\chi}^2 \rangle_f$  obtained by the analytical estimation and by the numerical calculation for  $\xi < 0, m_\chi = 0$  in the case of the  $R^4$  inflation model.

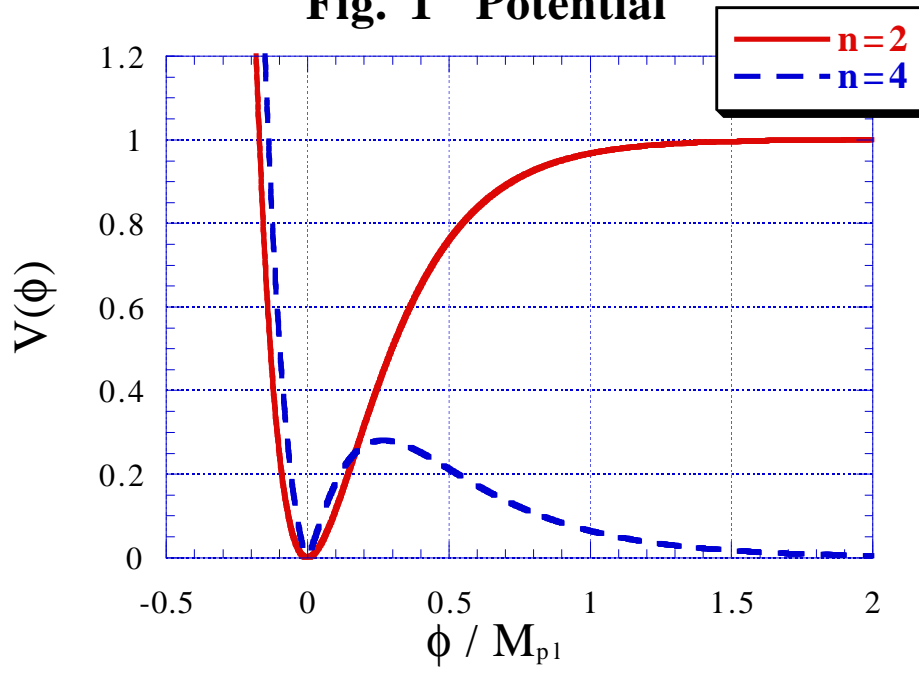
$\xi$	$\bar{t}_f$	$\langle \bar{\chi}^2 \rangle_{analytic}$	$\langle \bar{\chi}^2 \rangle_{numerical}$
-20	156	$1.13 \times 10^{-5}$	$3.08 \times 10^{-5}$
-30	130	$9.80 \times 10^{-6}$	$2.24 \times 10^{-5}$
-50	82	$1.18 \times 10^{-5}$	$2.18 \times 10^{-6}$
-70	65	$1.19 \times 10^{-5}$	$2.12 \times 10^{-5}$
-100	51	$1.20 \times 10^{-5}$	$2.30 \times 10^{-5}$
-300	36	$6.74 \times 10^{-6}$	$5.37 \times 10^{-6}$

## Figure Captions

- FIG. 1: The potential in the equivalent system to the  $R^n$  gravity theory. The solid and dotted curve denote the  $n = 2$  and  $n = 4$  cases respectively. The potential of the  $n = 2$  case is flat enough for  $\phi \gtrsim M_{\text{PL}}$  so that inflation occurs, but for the  $n > 2$  case, the potential has a local maximum at Eq. (2.9) and inflation is rather difficult to realize.
- FIG. 2: The schematic diagram of the Mathieu chart and the typical paths for two types of resonance. The lined regions denote the instability bands. Generally, The growth of  $\chi$  fluctuation terminates in two distinct ways. In the first case, when  $|\xi|$  is not so large, resonance ceases by universe expansion before  $\chi$ -particles are sufficiently produced. In this case, the increase of  $A_k$  due to  $\chi$ -particle production is negligible, and resonance stops when  $q$  drops down under unity (solid curve). In the second case, when  $|\xi|$  is as large as  $|\xi| \gtrsim 10$ , the growth of  $\chi$  fluctuation stops because of the increase of  $A_k$  due to  $\chi$ -particle production (dotted curve). In this case, resonance ends when the  $\chi$  field reaches the line  $A_k \approx 3q$  because few instability bands exist for  $A_k \gtrsim 3q$ .
- FIG. 3: The evolution of  $\langle \bar{\chi}^2 \rangle$  as a function of  $\bar{t}$  for  $\xi > 0, m_\chi = 0$  in the case of the  $R^2$  inflation model ((a)  $\xi = 3$ , (b)  $\xi = 5$ , and (c)  $\xi = 10$ ). We find that the parametric resonance occurs by the positive  $\xi$ -coupling.  $\langle \bar{\chi}^2 \rangle$  increases quasi-exponentially and reaches its final value  $\langle \bar{\chi}^2 \rangle_f$ . After then, it decreases by the adiabatic expansion.  $\langle \bar{\chi}^2 \rangle_f$  takes the maximal value when  $\xi \approx 5$ . For larger  $\xi$  ( $\xi \gtrsim 100$ ), although the growth rate becomes large, the final value  $\langle \bar{\chi}^2 \rangle_f$  is suppressed by  $\eta$  term.
- FIG. 4: The final value of  $\langle \bar{\chi}^2 \rangle$  as a function of  $\xi$  for  $m_\chi = 0$  in the case of the  $R^2$  inflation model. When  $\xi$  is positive,  $\langle \bar{\chi}^2 \rangle_f$  takes its maximal value  $\langle \bar{\chi}^2 \rangle_f = 1.74 \times 10^{-4}$  when  $\xi \approx 5$ . For  $\xi < 0$ ,  $\langle \bar{\chi}^2 \rangle_f$  takes its maximal value  $\langle \bar{\chi}^2 \rangle_{\text{max}} \approx 3 \times 10^{-4}$  when  $\xi \approx -4$  and  $\xi \approx -40$ , which is larger than the  $\xi > 0$  case.
- FIG. 5: The evolution of  $\langle \bar{\chi}^2 \rangle$  as a function of  $\bar{t}$  for  $\xi > 0, m_\chi = m$  in the case of the  $R^2$  inflation model ((a)  $\xi = 5$ , (b)  $\xi = 10$ , and (c)  $\xi = 20$ ). The growth of  $\langle \bar{\chi}^2 \rangle$  is suppressed by the mass of  $\chi$ -particles, especially when  $\xi$  is small. However, massive  $\chi$ -particles of the order  $m_\chi \sim 10^{13}$  GeV can be created sufficiently when  $\xi \gtrsim 10$ .
- FIG. 6: The final value of  $\langle \bar{\chi}^2 \rangle$  as a function of  $m_\chi$  for  $\xi = 100$  in the case of the  $R^2$  inflation model.  $\langle \bar{\chi}^2 \rangle_f$  is a quadratically decreasing function of  $m_\chi$ .  $\chi$ -particles whose mass is  $m_\chi \gtrsim 10m \sim 10^{14}$  GeV can not be produced, as is found by Eq. (3.12).
- FIG. 7: The evolution of  $\langle \bar{\chi}^2 \rangle$  as a function of  $\bar{t}$  for  $\xi < 0, m_\chi = 0$  in the case of the  $R^2$  inflation model ((a)  $\xi = -1$ , (b)  $\xi = -3$ , and (c)  $\xi = -5$ ). Since the value of  $|q|$  is larger as compared with the same absolute value of  $\xi$ , parametric resonance occurs even if  $\xi = -1$ . The value of  $\langle \bar{\chi}^2 \rangle_f = 2.63 \times 10^{-4}$  in the  $\xi = -5$  case is larger than the maximal value  $\langle \bar{\chi}^2 \rangle_f = 1.74 \times 10^{-4}$  in the positive  $\xi$  case. In the negative  $\xi$  case,  $\langle \bar{\chi}^2 \rangle_f$  takes maximal value  $\langle \bar{\chi}^2 \rangle_f \approx 3 \times 10^{-4}$  at  $\xi \approx -4$  and  $\xi \approx -40$ .
- FIG. 8: The evolution of  $\langle \bar{\chi}^2 \rangle$  as a function of  $\bar{t}$  for  $\xi < 0, m_\chi = m$  in the case of the  $R^2$  inflation model ((a)  $\xi = -5$  and (b)  $\xi = -10$ ). When  $\xi = -5$ , the mass effect significantly suppresses the final abundance. However, when  $\xi = -10$ , the mass effect of the order  $m_\chi = m$  does not play a relevant role. We find that massive  $\chi$ -particles of order  $m_\chi \sim 10^{13}$  GeV can be created sufficiently when  $\xi \lesssim -10$ .

- FIG. 9: The evolution of  $\langle \bar{\chi}^2 \rangle$  as a function of  $\tilde{t}$  for  $\xi > 0, m_\chi = 0$  in the case of the  $R^4$  inflation model ((a)  $\xi = 10$ , (b)  $\xi = 30$  and (c)  $\xi = 50$ ). We find that the parametric resonance occurs by the positive  $\xi$ -coupling. Since the initial fluctuation is small, the final value of  $\langle \bar{\chi}^2 \rangle$  is rather small for  $\xi = 10$ . However, in the case of  $\xi = 30$  and  $\xi = 50$ , the final value of  $\langle \bar{\chi}^2 \rangle$  reaches the value  $\langle \bar{\chi}^2 \rangle_f \sim 10^{-5}$ . For  $\xi \gtrsim 25$ ,  $\langle \bar{\chi}^2 \rangle_f$  does not increase because of the suppression effect due to  $\chi$ -particle production. As a result, in the  $\xi > 0$  case,  $\langle \bar{\chi}^2 \rangle_f$  takes almost constant value:  $(1 \sim 3) \times 10^{-5}$  for  $25 \lesssim \xi \lesssim 100$ .
- FIG. 10: The final value of  $\langle \bar{\chi}^2 \rangle$  as a function of  $\xi$  for  $m_\chi = 0$  in the case of the  $R^4$  inflation model.  $\langle \bar{\chi}^2 \rangle_f$  takes almost constant value  $\langle \bar{\chi}^2 \rangle_f \approx (1 \sim 5) \times 10^{-5}$  for  $20 \lesssim |\xi| \lesssim 100$ . The maximal value of  $\langle \bar{\chi}^2 \rangle_f$  is  $\langle \bar{\chi}^2 \rangle_{max} \approx 5 \times 10^{-5}$  at  $\xi \approx -35$ .
- FIG. 11: The evolution of  $\langle \bar{\chi}^2 \rangle$  as a function of  $\tilde{t}$  for  $\xi < 0, m_\chi = 0$  in the case of the  $R^4$  inflation model ((a)  $\xi = -5$ , (b)  $\xi = -20$  (c)  $\xi = -50$ ). When  $\xi = -5$ , parametric resonance evidently occurs, but the final value of  $\langle \bar{\chi}^2 \rangle$  is rather small. However, in the case of  $\xi \lesssim -20$ ,  $\chi$ -particles are sufficiently produced. For  $-100 \lesssim \xi \lesssim -20$ ,  $\langle \bar{\chi}^2 \rangle_f$  takes almost constant value  $\langle \bar{\chi}^2 \rangle_f \approx (2 \sim 5) \times 10^{-5}$ .
- FIG. 12: The evolution of  $\langle \bar{\chi}^2 \rangle$  as a function of  $\tilde{t}$  for  $\xi = -50, m_\chi = m_4$  in the case of the  $R^4$  inflation model. As compared with the massless case,  $\langle \bar{\chi}^2 \rangle$  is strongly suppressed by the mass effect. Generally, massive  $\chi$ -particles which do not satisfy the condition Eq. (4.13) can not be created.

**Fig. 1 Potential**





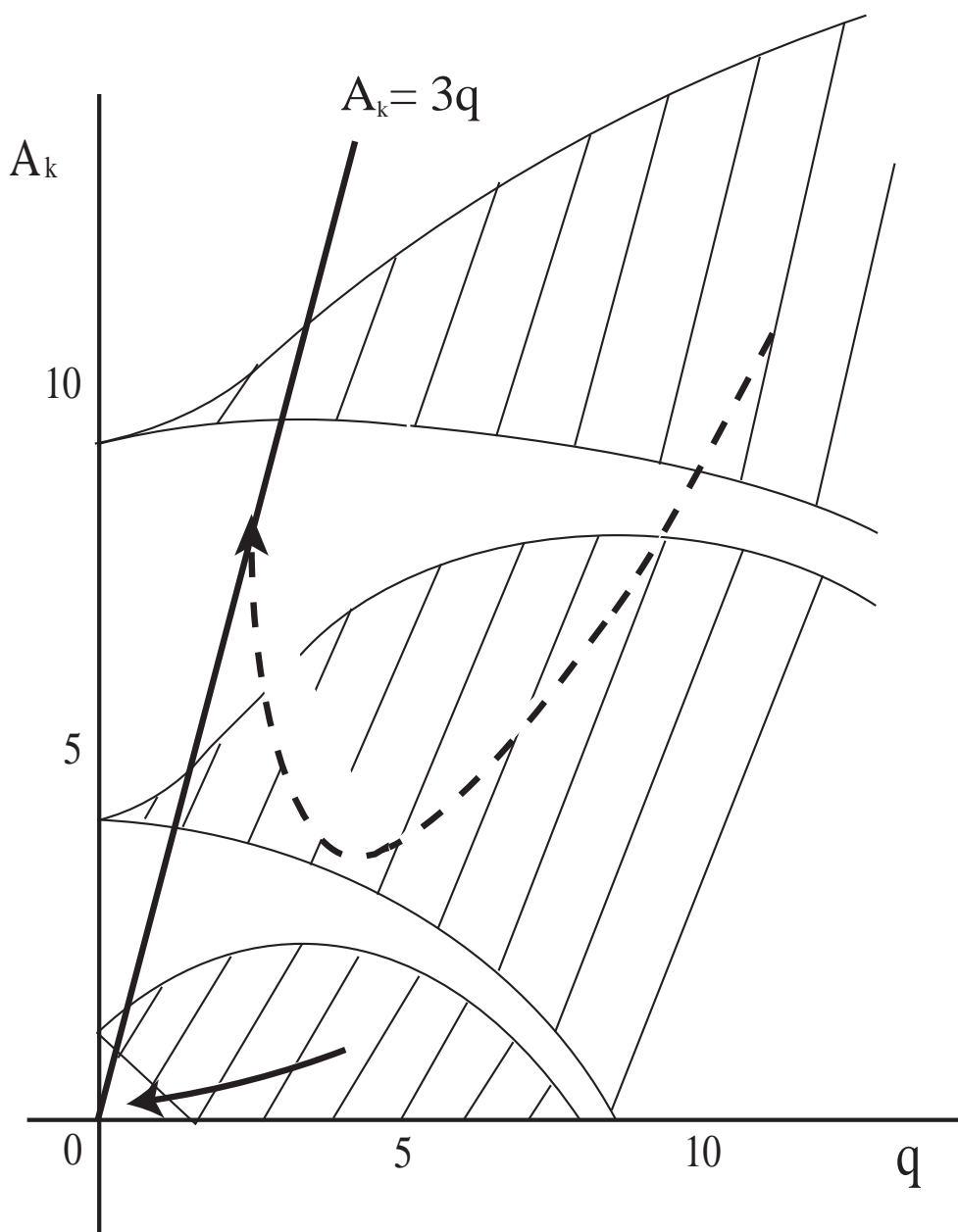
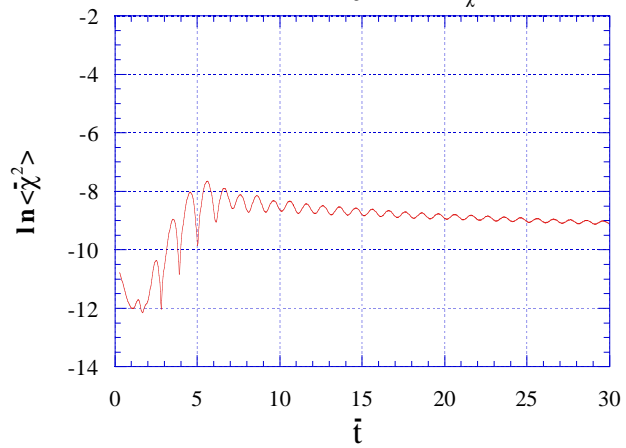
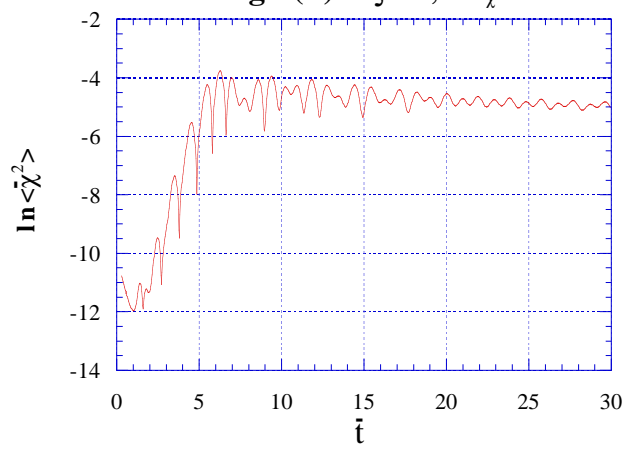


Fig. 2

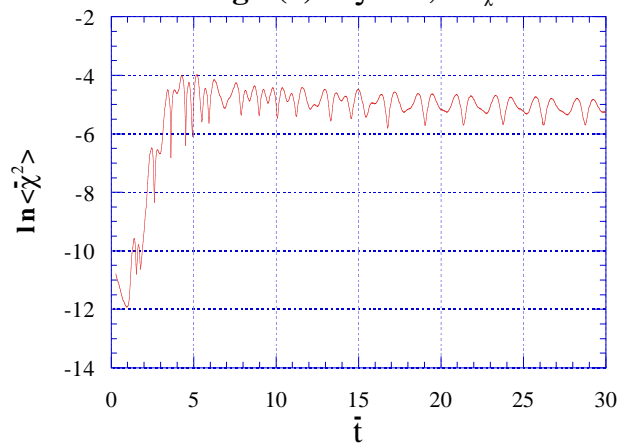
**Fig.3(a)**  $\xi = 3, \mathbf{m}_\chi = \mathbf{0}$



**Fig.3(b)**  $\xi = 5, \mathbf{m}_\chi = \mathbf{0}$

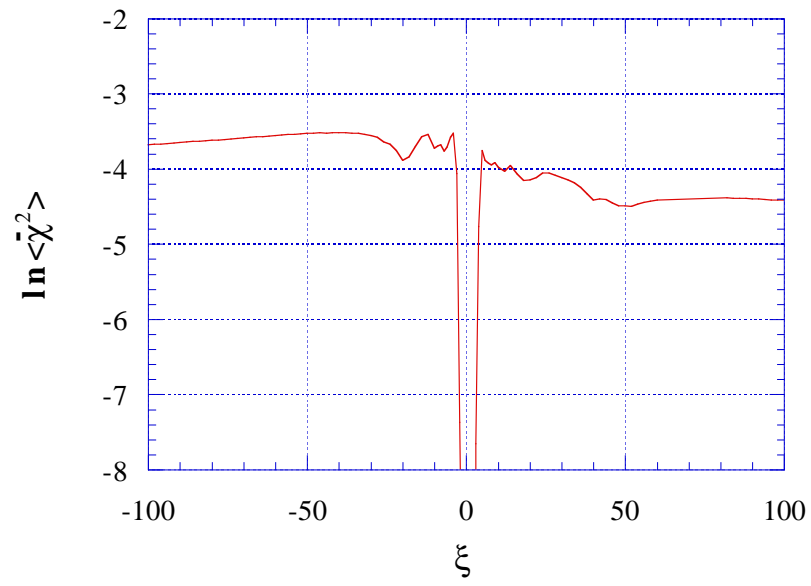


**Fig.3(c)**  $\xi = 10, \mathbf{m}_\chi = \mathbf{0}$

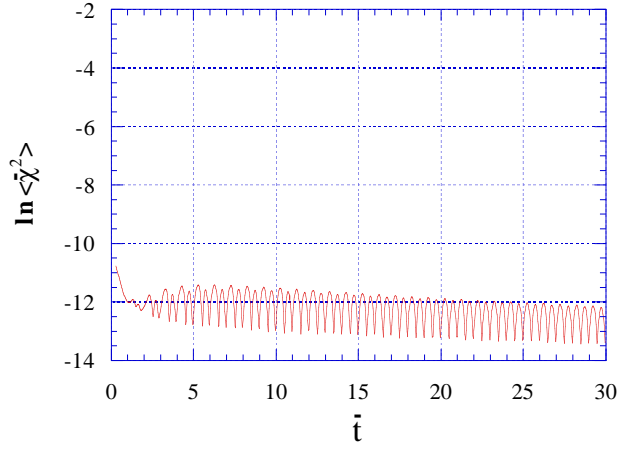




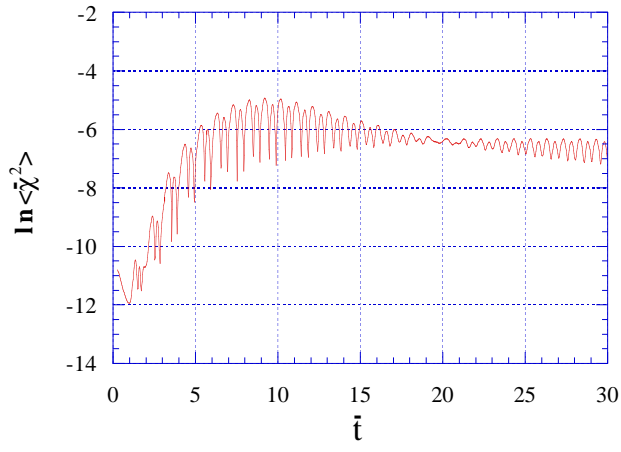
**Fig. 4**  $\xi - \langle \chi^2 \rangle$  relation



**Fig.5(a)**  $\xi=5, \mathbf{m}_\chi=\mathbf{m}$



**Fig.5(b)**  $\xi=10, \mathbf{m}_\chi=\mathbf{m}$



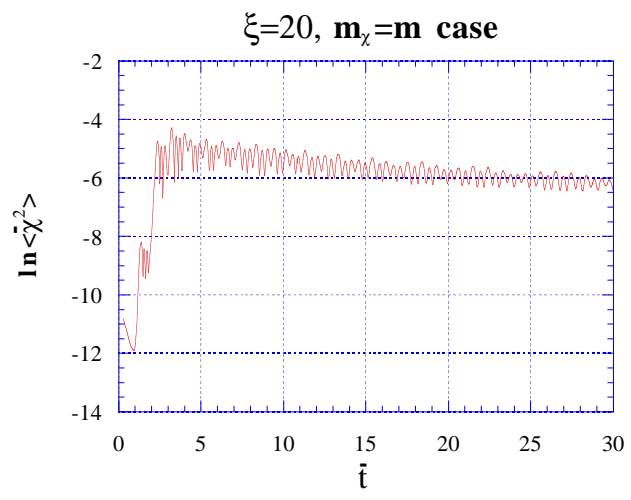


**Fig. 6  $\mathbf{m}_\chi$  -  $\langle \chi^2 \rangle_f$  relation**

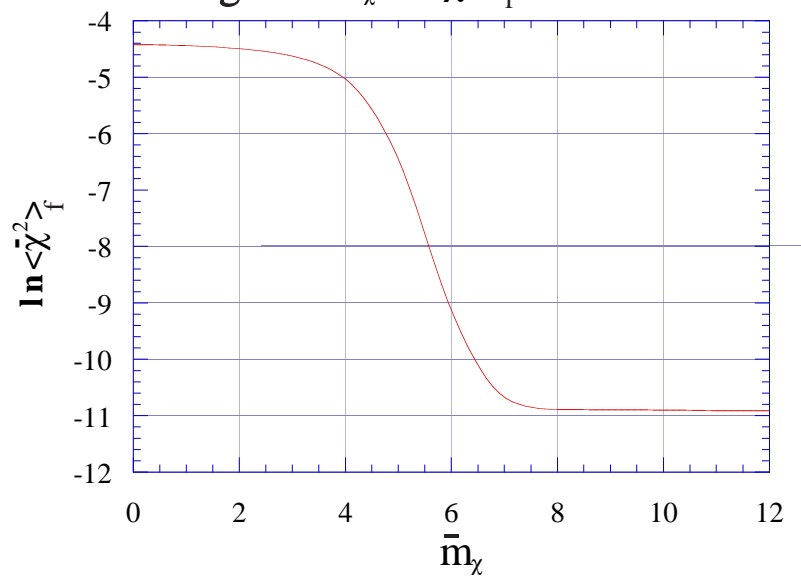


**Fig.7(a)**  $\xi = -1, m_\chi = 0$

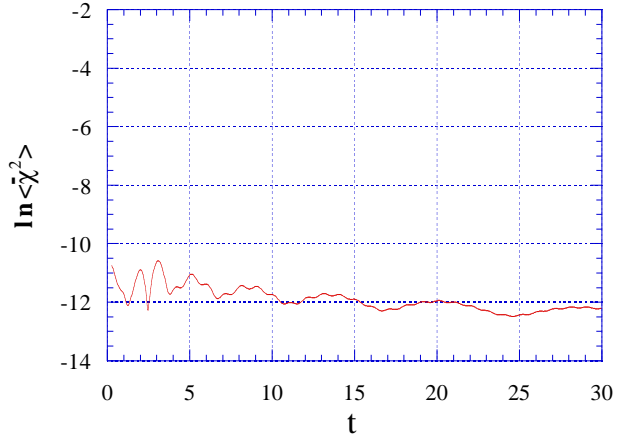


**Fig.7(b)**  $\xi = -3, m_\chi = 0$

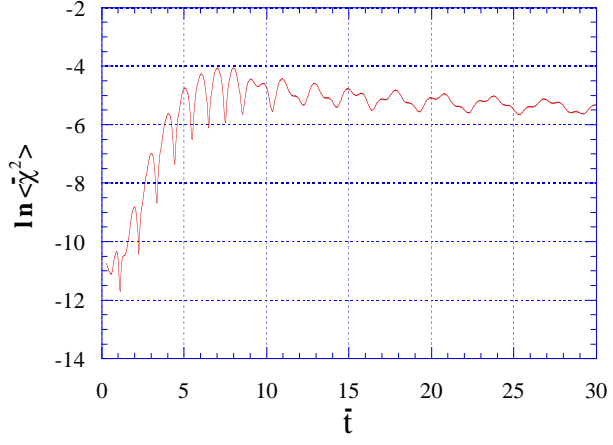


**Fig.7(c)**  $\xi = -5, m_\chi = 0$

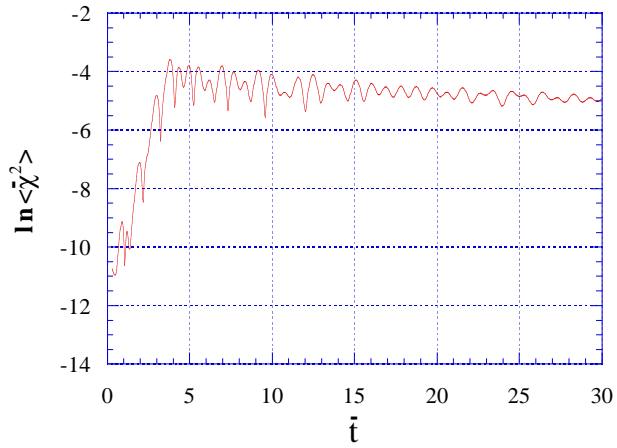






**Fig.8(a)**  $\xi = -5, m_\chi = m$

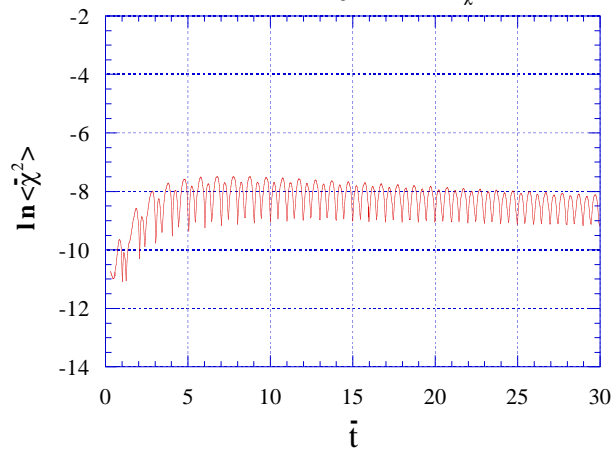


**Fig.8(b)**  $\xi = -10, m_\chi = m$

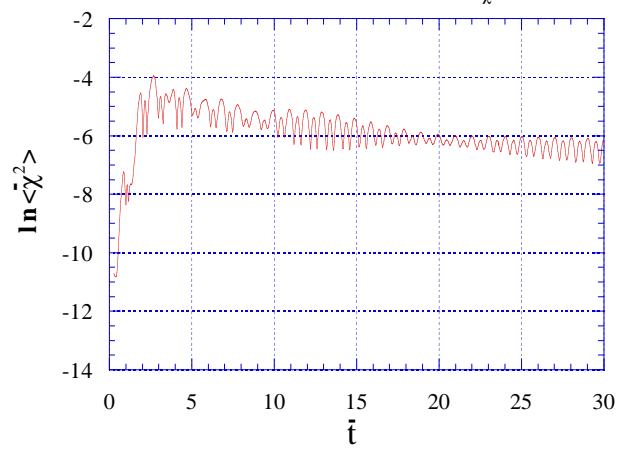


**Fig.9(a)**  $\xi=10, m_\chi=0$

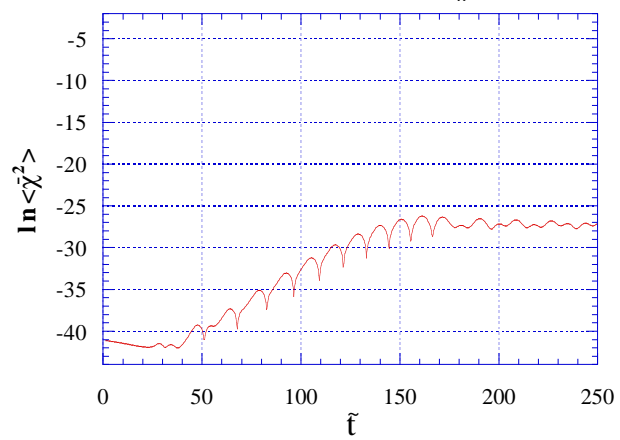


**Fig. 9(b)**  $\xi=30, m_\chi=0$

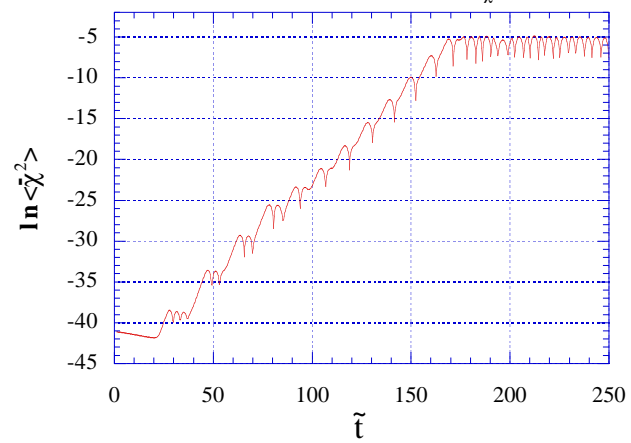


**Fig.9(c)**  $\xi=50, m_\chi=0$

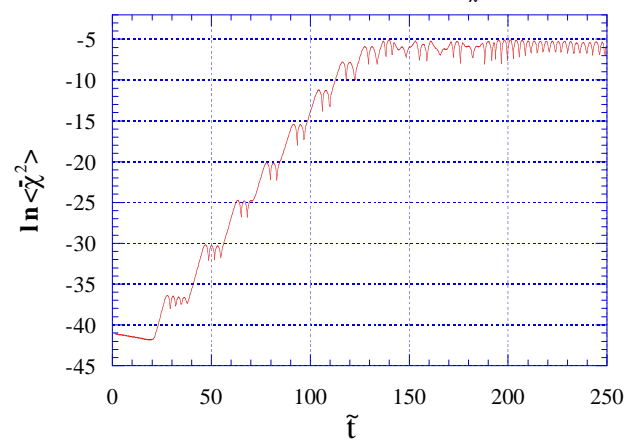




**Fig. 10**  $\xi - \langle \chi^2 \rangle$  relation

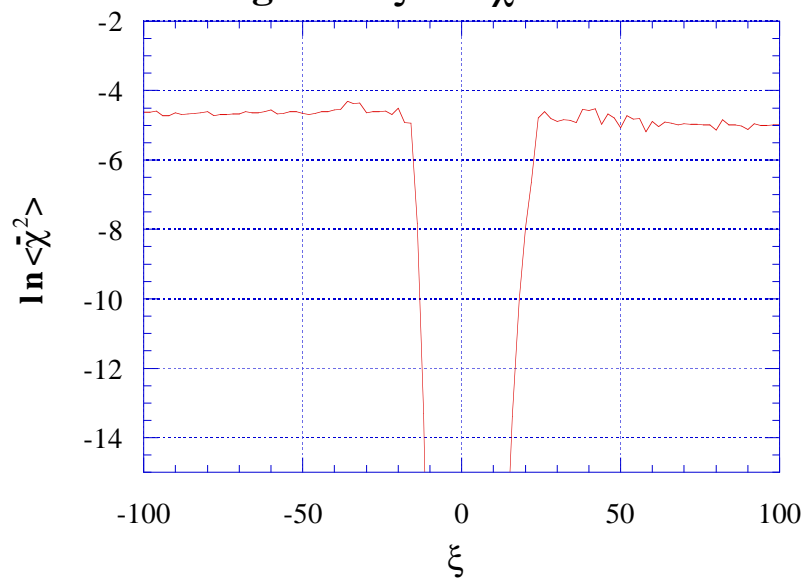


**Fig.11(a)**  $\xi = -5, m_\chi = 0$

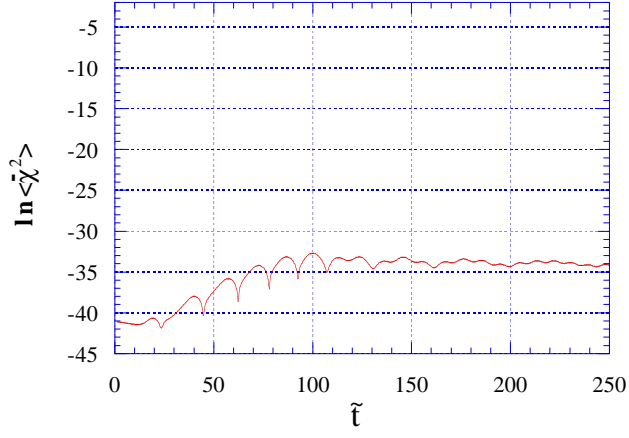


**Fig. 11(b)**  $\xi = -20, m_\chi = 0$

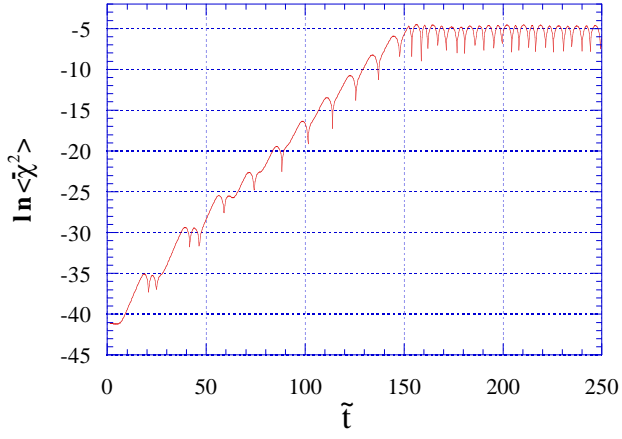


**Fig. 11(c)**  $\xi = -50, m_\chi = 0$

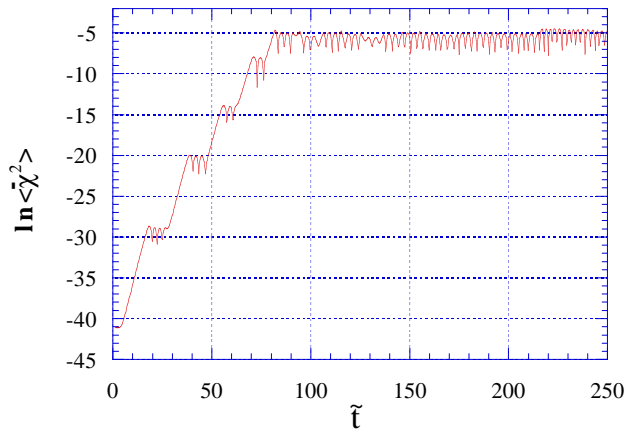




**Fig. 12**  $\xi = -50$  ,  $m_\chi = m_4$

